Kinetic sculpting of the seven stripes of the *Drosophila even-skipped* gene

Augusto Berrocal[1,*], Nicholas Lammers[2,*], Hernan G. Garcia[1,2,3,4,$] and Michael B. Eisen[1,2,4,5,6,$]

1. Department of Molecular & Cell Biology, University of California at Berkeley, Berkeley, California
2. Biophysics Graduate Group, University of California at Berkeley, Berkeley, California
3. Department of Physics, University of California at Berkeley, Berkeley, California
4. Institute for Quantitative Biosciences-QB3, University of California at Berkeley, Berkeley, California
5. Department of Integrative Biology, University of California at Berkeley, Berkeley, California
6. Howard Hughes Medical Institute

* co-first authors
$ joint senior authors

Direct correspondence to: mbeisen@berkeley.edu

Abstract

We used live imaging to visualize the transcriptional dynamics of the *Drosophila melanogaster even-skipped* gene at single-cell and high temporal resolution as its seven stripe expression pattern forms, and developed tools to characterize and visualize how transcriptional bursting varies over time and space. We find that despite being created by the independent activity of five enhancers, *even-skipped* stripes are sculpted by the same kinetic phenomena: a coupled increase of burst frequency and amplitude. By tracking the position and activity of individual nuclei, we show that stripe movement is driven by the exchange of bursting nuclei from the posterior to anterior stripe flanks. Our work provides a conceptual, theoretical and computational framework for dissecting pattern formation in space and time, and reveals how the coordinated transcriptional activity of individual nuclei shape complex developmental patterns.

Introduction

The patterns of gene expression that choreograph animal development are formed dynamically by an interplay between processes - transcription, mRNA decay and degradation, diffusion, directional transport and the migration of cells and tissues - that vary in both space and time. However the spatial aspects of transcription have dominated the study of developmental gene expression, with the role of temporal processes in shaping patterns receiving comparably little attention (J. Bothma and Levine 2013; Garcia et al. 2020).

Gene expression patterns are dynamic on many levels. They form, change and disappear over time, often as cells, tissues and organs are forming and moving in the developing embryo (Lawrence 1992). Furthermore the transcriptional process that creates these patterns is itself highly dynamic. The classical view of transcription as a switch or a tunable rheostat has been replaced in recent years by the recognition that mRNA synthesis occurs in bursts, with promoters switching stochastically between an ON state where polymerases are loaded and begin elongating, and an OFF state where few or no new transcripts are initiated (Figure 1A) (Zenklusen, Larson, and Singer 2008; Golding et al. 2005; Blake et al. 2006; Janicki et al. 2004; Chubb et al. 2006; Yunger et al. 2010; Raj et al. 2006; Lionnet et al. 2011; Muramoto et al. 2012; Little, Tikhonov, and Gregor 2013; Xu et al. 2015; Lenstra et al. 2015; Fukaya, Lim, and Levine 2016; Desponds et al. 2016; Hendy et al. 2017a; Lammers et al. 2020).

A slew of studies, from theoretical models (Ko 1991; Peccoud and Ycart 1995; Sánchez and Kondev 2008; Sanchez et al. 2011; Xu et al. 2016; Choubey, Kondev, and Sanchez 2015, 2018; Shahrezaei and Swain 2008; Kepler and Elston 2001; Sasai and Wolynes 2003) to imaging-based analyses (Xu et al. 2015; Fukaya, Lim, and Levine 2016; Senecal et al. 2014; Jones, Brewster, and Phillips 2014; Golding et al. 2005; Molina et al. 2013; Suter et al. 2011; So et al. 2011; Padovan-Merhar et al. 2015; Bartman et al. 2016; Hendy et al. 2017b; Zoller, Little, and Gregor 2018), have shown that overall rates of mRNA synthesis can be adjusted by controlling the bursting process. Changing the duration or bursts, the separation between bursts, or the rate at which polymerases are loaded during a burst (Figure 1B) will affect mRNA production, and modulating any or all of these parameters over space and time could, in principle, produce arbitrarily complex output patterns. However, it remains unclear how diverse the kinetic strategies employed by different regulatory sequences actually are, and what, if anything, constrains how these different kinetic parameters are used by evolution to shape patterns of expression.

In this paper we set out to compare the ways in which different enhancers that drive similar types of spatiotemporal patterns during animal development deploy transcriptional bursting to produce their outputs by examining transcription at the single-cell level in living embryos. We use as our model the *Drosophila melanogaster even-skipped* (*eve*) gene whose seven stripes ring the embryo in the cellularizing blastoderm (nuclear cycle 14; nc14) in the hour preceding gastrulation (Surkova et al. 2008; Fowlkes et al. 2008; Jiang et al. 2015; Ludwig et al. 2011; Macdonald, Ingham, and Struhl 1986; Frasch and Levine 1987).

The *eve* stripes are produced through the largely independent activity of five discrete enhancers (Figure 1C) that drive individual stripes (the stripe 1, stripe 2, and stripe 5 enhancers) or pairs of stripes (the stripe 3/7 and stripe 4/6 enhancers) (Harding et al. 1989; Goto, Macdonald, and Maniatis 1989; Small et al. 1991). These enhancers respond in different ways to canonical maternal factors Bicoid (Bcd) and Caudal (Cad), and gap genes Hunchback (Hb), Giant (Gt), Krüppel (Kr), Knirps (Kni) and Sloppy Paired 1 (Slp1), among others, balancing activating and repressive inputs to generate novel output patterns (Mannervik 2014). For example, the *eve* stripe 2 enhancer is activated in the anterior by Bcd and Hb, and repressed by Gt and Kr, ultimately expressing in a stripe of nuclei that fall between the domains occupied by these two repressors (Frasch and Levine 1987; Small, Blair, and Levine 1992).

Transcriptional bursting is widespread during *D. melanogaster* development (Little, Tikhonov, and Gregor 2013; Xu et al. 2015; J. P. Bothma et al. 2014; Fukaya, Lim, and Levine 2016; Boettiger and Levine 2013; Holloway and Spirov 2017; Zoller, Little, and Gregor 2018; Paré et al. 2009; Lammers et al. 2020). For example, (J. P. Bothma et al. 2014) utilized the MS2 system, which exploits the interaction between the phage MS2 coat protein (MCP) and a short RNA stem loop to fluorescently label nascent transcripts as they are being synthesized (Bertrand et al. 1998; Garcia et al. 2013; Forrest and Gavis 2003), to directly visualize and quantify transcription from an *eve* stripe 2 transgene at single nucleus resolution. They showed that the stripe is generated by bursts of transcriptional activity in the nuclei that form it, and that the aggregate pattern is highly dynamic, forming and dissipating rapidly during nc14.

Our objective in carrying out this work was twofold: first, to characterize the detailed dynamics of this classical and well-studied pattern as a means to reveal how multiple enhancers dictate potentially distinct bursting dynamics to shape a gene expression in the embryo, and second, to establish a rigorous systematic framework for analyzing such data, and conceptual paradigms for characterizing what we observe from this new type of experiment. Indeed, the advent of live imaging in the context of development calls for the establishment of a new

language and new metrics for characterizing the formation of gene expression patterns in space and time.

We use a variety of new analyses to generate a kinetic fingerprint of *eve* transcription during stripe formation - a record of temporal and spatial variation in the bursting state of the promoters of ~3,000 nuclei covering all seven stripes throughout nc14 - and to visualize different aspects of *eve* regulation. We find that all seven *eve* stripes are sculpted by the same regulatory strategies: the elimination of new bursts between stripes; the enhancement of bursting across stripes through a coupled increase in k_{on} and r; and the refinement and movement of stripe positions by the addition of bursting nuclei along the anterior edge of the stripes and the loss of bursting along their posterior edge.

Thus, in this experiment and with our new set of analytical tools, we capture not only how single cell transcriptional activity encodes the formation of the stripes, but also how this activity is modulated in space and time in order to create and displace a complex pattern of gene activity across the embryo.

Results

Live imaging of *eve* expression

We used recombineering (Warming et al. 2005) to modify a bacterial artificial chromosome (BAC) (Venken et al. 2006) containing the *D. melanogaster eve* gene and all of its enhancers and regulatory elements (Venken et al. 2009), replacing the coding region with an array of MS2 stem loops followed by the *D. melanogaster yellow* (*y*) gene (Figure 1D; (J. P. Bothma et al. 2014)). The 4,329 base pair *y* gene, which is longer than the endogenous *eve* transcript, is phenotypically neutral and provides a means to increase the number of RNA Polymerase II (Pol II) molecules loaded onto the gene in order to amplify the signal (see Methods for a discussion of how the structure of the reporter genes affects the fluorescence signal, analyses and inferences performed throughout this work). We inserted the engineered BAC into a targeted site on chromosome 3L using ΦC31 integrase-mediated recombination (Fish et al. 2007), and homozygosed the line, which showed no signs of adverse effects of the transgene.

We crossed males from this line with females carrying transgenes that express in embryos an RFP-labeled histone to visualize nuclei, and an MCP-GFP fusion that binds the MS2 RNA stem loops. The result is the direct visualization and quantification of nascent transcripts at the transgene locus as fluorescent puncta (Garcia et al. 2013). The temporal and spatial pattern of

eve transgene transcription recapitulates the well-characterized dynamics of *eve* expression, most notably formation of the characteristic seven stripes in the late blastoderm (Figure 2; Video 1; (Surkova et al. 2008; Fowlkes et al. 2008; Jiang et al. 2015; Ludwig et al. 2011)). Further, as recently demonstrated in (Lammers et al. 2020) this BAC reporter construct quantitatively recapitulates the cytoplasmic *eve* mRNA pattern as measured by FISH (Lammers et al. 2020; Luengo Hendriks et al. 2006)(Lim et al. 2018).

We used laser-scanning confocal microscopy to record, with high temporal resolution and high magnification, two color (MCP-GFP and histone RFP) movies of embryos from before nc14 through gastrulation. We optimized our data collection strategy to sample multiple stripes (three to five) in each movie, to obtain high temporal resolution (one Z-stack, corresponding to each time point of our movies, every 16.8 seconds) and to have optimal signal to noise with minimal bleaching. In total, we collected 11 movies (Videos 2-12), with every stripe imaged at least five times (see Table 1).

We used a custom image processing pipeline (Garcia et al. 2013; Lammers et al. 2020) to identify nuclei, track fluorescent puncta and extract fluorescence intensities in each nucleus over time. The resulting data (File S1) contains fluorescence traces from 2,961 nuclei at an interpolated time interval of 20s, representative examples of which are shown in Figure 3A.

We first sought to reexamine the previously characterized temporal dynamics of stripe formation (Surkova et al. 2008; Fowlkes et al. 2008; Jiang et al. 2015; Ludwig et al. 2011) using the increased temporal resolution (relative to earlier analyses of fixed embryos and of slowly maturing fluorescent protein reporters) of these data (Figure 3B). Early imaging studies described *eve* as being expressed broadly in nc13 and early nc14 embryos before refining sequentially into four, then seven stripes (Macdonald, Ingham, and Struhl 1986; Frasch and Levine 1987). Subsequent work with improved labeling and imaging techniques (Surkova et al. 2008; Fowlkes et al. 2008) revealed an initial phase with broad domains in the anterior and posterior, followed by the formation of stripes from within these broad domains and, eventually, amplification of the stripe pattern.

During nc14, we first observe *eve* transcription beginning approximately five minutes after the onset of anaphase. The initial transcription covers a broad swath of the embryo, from around 25% to 75% egg-length, with the highest activity in two domains roughly centered in the anterior and posterior halves of the embryo respectively. The greatest fluorescence signal during the first 25 minutes of nc14, when stripes are not yet fully formed, is in the most anterior region of *eve* transcription, in an area in which stripe 1 will eventually form.

Although the full seven stripe pattern is not fully formed until around 25 minutes, the three anterior-most stripes are already apparent as locally high areas of fluorescence intensity as early as 10 minutes. By 20 minutes stripes 1, 2 and 3 have clearly separated from background, stripes 4 and 6 appear to split off from a large posterior domain, and stripe 7 forms *de novo* in the posterior. Stripe 5 appears as a distinct stripe last, emerging in an area of low transcriptional activity left behind following the splitting of stripes 4 and 6. The stripes persist for the remainder of nc14, gradually increasing in fluorescence intensity until they reach a peak at around 35 minutes into nc14.

The positions of stripes 1-3 along the anterior-posterior (AP) axis are largely stable after they form, while stripes 4-6 show small anterior shifts. Stripe 7 makes a more dramatic movement towards the anterior, moving approximately 8% of egg-length, or around 40 μm from its initial location. The quantitative characterization of this stripe movement, the decoupling between stripes and nuclei, and the quantification of transcriptional bursting dynamics in each nucleus necessitated the development of a method, described below, to dynamically define the position of stripes throughout each movie.

Modeling and inference of promoter state

As expected, the fluorescence traces from individual nuclei show clear hallmarks of transcriptional bursting, with apparent stochastic fluctuations between states with low and high fluorescence output (Figure 3A). Following previous work in the field (Golding et al. 2005; Chubb et al. 2006; Zenklusen, Larson, and Singer 2008; Lionnet et al. 2011; Muramoto et al. 2012; Little, Tikhonov, and Gregor 2013; Xu et al. 2015; Lenstra et al. 2015; Fukaya, Lim, and Levine 2016; Desponds et al. 2016; Hendy et al. 2017a; Zoller, Little, and Gregor 2018; J. P. Bothma et al. 2014; Paré et al. 2009; Lim et al. 2018), we model bursting as a simple Markovian process in which a promoter switches stochastically between an OFF and an ON state with rates k_{on} and k_{off}. When the promoter is in the ON state, we assume it loads polymerases continuously with a constant rate r (Figure 1A).

In our implementation of the MS2 system, once a polymerase molecule transcribes the stem loops located at the 5' end of the gene, the MCP-GFP molecules bound to the stem loops produce a constant fluorescent signal at the locus that persists until this polymerase completes its traversal of the gene. Building off of the method presented in (Lammers et al. 2020), we estimated this polymerase transit time as the displacement that gives the minimum value in the autocorrelation of the single frame differences in the fluorescent signal (see Methods). The

rationale for this approach was that every increase in signal due to polymerase loading at time t should be accompanied by a corresponding decrease in signal at time $t+t_{elong}$ due to the completion of a transcriptional elongation cycle with a delay equal to the elongation time (Coulon and Larson 2016; Desponds et al. 2016). We arrived at an estimate of 140s (Figure 4A), consistent with a direct measurement of the rate of polymerase elongation of ~2,700 bp/min from (Fukaya, Lim, and Levine 2017) and the length of the construct (6,563bp).

We model the bursting process at each promoter in discrete time steps of Δt = 20s, set by the time resolution of our imaging. Under our model, in each time window a promoter is either OFF and not loading polymerases, or ON and loading polymerases at a fixed rate. A promoter that is in the ON state loads Δt x r polymerases, producing a single pulse of fluorescence proportional to Δt x r (with the proportionality factor determined by the fluorescence of GFP and the fraction of MS2 loops bound by MCP-GFP). This pulse lasts at the locus for 140s, at which point all polymerase molecules loaded during the original time window have terminated transcribing (Figure 4B). Since we do not calibrate the fluorescence signal to the number of polymerase molecules for this construct, in practice we fold the proportionality factor into r altering its units from polymerases loaded per unit time to fluorescence signal produced per unit time. Since many transcriptional bursts last for longer than 20s, the fluorescence output of a single burst is a sum of the pulses generated during each time window.

In the embryos we imaged here, the MS2 BAC is heterozygous, contributed only by the father, while the mother contributes the MCP-GFP. However DNA replication occurs within an average of 10 mins for loci in nc14 (McKnight and Miller 1977; Rabinowitz 1941; Shermoen, McCleland, and O'Farrell 2010), meaning that there are actually two sister chromatids with the MS2 containing transgene in every nucleus. Because of sister chromatid cohesion, we can not, in general, discriminate both copies (Fung et al. 1998; Wilkie et al. 1999; Little, Tikhonov, and Gregor 2013). As it is still unclear how the sister chromatids influence each other's transcription (McKnight and Miller 1977; Lammers et al. 2020; Zoller, Little, and Gregor 2018), we model the locus as having two independent promoters that operate independently but governed by the same bursting parameters. Thus the system can be in one of three states: OFF, one promoter ON, and two promoters ON (Figure 4B).

If we know the state of the promoter over time, we can reconstruct its expected fluorescence output by summing 140s pulses beginning at each point where the promoter is ON and having height r if one promoter is ON or height 2 x r if two promoters are ON (Figure 4C). Traces modeled from hypothetical promoter state sequences (Figure 4C) have the features of the

observed fluorescence signal: linear increases in intensity (corresponding to periods when the promoter is ON); plateaus (corresponding to periods when transcriptional initiation is matched with previously initiated polymerases completing their transit of the gene); and linear signal decays (corresponding to periods when the promoter is OFF but previously initiated polymerases are still transiting the gene) (J. P. Bothma et al. 2014; Garcia et al. 2013).

However, when given a fluorescence trace, it is not trivial to infer the promoter state sequence that generated it, owing to the time convolution between promoter state and fluorescence output. To solve this problem, we developed a compound state hidden Markov model (cpHMM, described in (Lammers et al. 2020)) that estimates global parameters k_{on}, k_{off}, and r for a set of traces, and allows us to identify the maximum-likelihood promoter state sequence under these parameters for every trace via the Viterbi algorithm.

The cpHMM thus accomplishes two aims central to treating these data in a more rigorous and biologically meaningful manner. First, it allows us to describe the bursting behavior of any set of nuclei in quantitative terms. Across all seven stripes, the model infers approximate k_{on} k_{off} values of 0.60 events per minute and an r of 67 AU per minute. And second, by providing a means to fit a sequence of ON and OFF states to the data from each nucleus, the cpHMM allows us to shift the focus in the analysis of individual traces from fluorescence, which only indirectly reflects the temporal behavior of a promoter, to the instantaneous promoter state (Figure 4D-F; see also File S1 which the inferred promoter state for each nucleus at every time point and the corresponding modeled fluorescence intensity, and Videos 13-23).

Dynamic determination of stripe positions

Before analyzing the data further we had to solve two practical problems. To compare the kinetic behavior of individual stripes, we had to determine which nuclei were in each stripe at every time point, a process complicated by the movement of stripes relative to both the embryo and nuclei. Further, to analyze the data *in toto*, we also had to register the 11 movies relative to each other and to the embryo.

To address these challenges, we used a Gaussian mixture model to cluster bursting nuclei in each movie in a series of overlapping six-minute time windows based on their x and y positions in the image (Figure 5A). This clustering reliably separates nuclei into individual stripes. We next determined the orientation of each stripe to the AP and imaging axes by fitting a line to coordinates of all nuclei assigned to that stripe in each movie (Figure 5B). We fit a line with this slope to bursting nuclei from each time window (Figures 5C and 5D), and use these fits

to generate a linear model of the position of each stripe in each image over time, which we use to reorient the stripe so that it is perpendicular to the image x-axis (Figure 5E).

We next use the known coordinates of the anterior and posterior poles of the embryo to convert the image x-axis to AP position, and register the examples of each stripe from different movies by setting the AP position of the center of each stripe at 35 min in nc14 to the mean AP position of all examples of that stripe at 35 min, adjusting the position of the stripe at other time points by the same correction (Figure 5F). As the stripes are not all present until after 25 min in nc14, we assign and register nuclei before that point based on the stripe position at 25 min. The stripe assignment is invariant over bootstrapping of movies, and the standard deviation of the AP displacement over bootstrapping of movies is 0.0016.

Collectively these data represent an easy to visualize and interpret kinetic fingerprint of stripe formation: a record of every transcriptional burst that occurred during the formation of *eve* stripes in these embryos (Figure 6; Video 24).

Bursting dynamics of individual nuclei

We used the output of the cpHMM and registration process to examine the locations of transcriptional bursts along the AP axis and over time (Figure 6). The most striking feature is the almost complete lack of observable transcriptional bursts in the regions between stripes from 25 minutes into nc14, with the exception of the 5-6 interstripe which is discussed below (note that this is not an artifact of the movie alignment and orientation process, as this effect is seen clearly in individual movies). We took advantage of the fact that we were tracking bursts in individual nuclei in order to analyze the relationship between this absence of bursting in interstripe regions and the single-nucleus bursting behavior within stripes.

Stripes are defined by sharp spatial boundaries, with the transition between the low bursting (quiescent) state and the frequently bursting (active) state occurring from one column of nuclei to the next (Figure 6), consistent with the classical descriptions of *eve* stripe patterns (Small et al. 1991; Frasch and Levine 1987; Fujioka et al. 1999; Small, Blair, and Levine 1992; Warrior and Levine 1990; Clyde et al. 2003). They also have sharp temporal boundaries: all of the interstripe regions, save that between stripes 6 and 7, form in regions where there was appreciable bursting early in nc14 that disappears at around 25 minutes into the nuclear cycle (Figure 6).

To better understand how the low-bursting state in interstripes is established, we looked at the bursting history of the nuclei in these regions (Figure 7). The first feature we noticed was

that most of the nuclei that ultimately form the interstripe were never detected to burst at any point in nc14 (Figure 7A,B). With the exception of the 5-6 interstripe, these never-ON nuclei effectively form the boundaries between stripes, as essentially every nucleus within each stripe bursts at some point during nc14 (Figure 7A,B).

The contrast in bursting history between stripes and interstripes is less pronounced in the posterior, where there are fewer such never-ON nuclei in the interstripe region (Figure 7B, notice the lower density of red single-nuclei tracks corresponding to never-ON nuclei). In order to reveal the source of this reduced number of never-ON nuclei in posterior interstripes, we analyzed their bursting history. Figure 7C shows the AP positions of the nuclei in one movie covering stripe 7 as a function of time, with the period in which they are part of the stripe highlighted. Although the stripe is clearly present throughout this period, no nuclei remain a part of the stripe for the entirety of this 25 minute period. As time progresses, nuclei at the posterior edge of stripe 7 shift from an active state, in which the promoter stochastically alternates between the ON and OFF transcriptional states, to a quiescent state in which we observe no subsequent bursting. In contrast, nuclei just off the anterior edge of the stripe switch from a quiescent to an active state at roughly the same rate. This leads to a net overall anterior movement of the stripe, akin to treadmilling, at a velocity of approximately one percent of embryo length every three minutes.

Consistent with (Lim et al. 2018), the other stripes exhibit smaller and varied anterior shifts (Figure 7-S1), but in every case the shift is associated with a similar coupled gain of active nuclei along the anterior edge and loss along the posterior edge. This effect is most clearly seen in Figure 7D, which shows, for each time point where a nucleus initiates a new burst, the difference in activity (defined as the difference between the fraction of the time the nucleus is in the ON state in the subsequent 10 min minus the fraction of the time the nucleus is in the ON state in the preceding 10 min). For all seven stripes there is a clear spatial pattern, with nuclei along the anterior edge of the stripe entering a bursting state and blue nuclei along the posterior edge becoming quiescent, indicating a movement of stripes relative to nuclei. Hence, stripe movement is associated with the dynamic switch of nuclei between active and quiescent states and not just with the movement of nuclei themselves.

<u>All seven *eve* stripes are created by the same regulation of bursting kinetics</u>

We next turned to the questions of how the spatial pattern of nuclear transcriptional activity described above is produced by regulating bursting kinetics, and whether this regulation differs among the seven *eve* stripes. In principle, any pattern of transcriptional activity could be achieved by modulating the duration, separation and/or amplitude of bursts across space and time. For example, a stripe could be created by varying burst separation along the anterior-posterior axis, with nuclei in the stripe center having lower burst separation, and those outside the stripe having long periods without bursts, or no burst at all. Alternatively, the same stripe could be created with uniform burst separation across nuclei, but elevated burst duration or amplitude within the stripe, or by modulating multiple parameters simultaneously.

Ideally, we would like to have a measure of the bursting parameters governing the behavior of every nucleus. However, individual MS2 traces have too few time points to allow for accurate cpHMM inference of burst parameters at the single trace level. We therefore used the cpHMM to infer k_{on}, k_{off}, and r for groups of nuclei binned on their mean fluorescence output and stripe. The logic of the fluorescence binning was that, given that $<fluorescence> \propto r\frac{k_{on}}{k_{on}+k_{off}}$ (Lammers et al. 2020), nuclei that have similar k_{on}, k_{off}, and r will have similar fluorescence outputs. Our inference shows that k_{on} is very strongly regulated as a function of average fluorescence in a consistent manner across stripes (Figure 8A). In contrast, only a weak drop in k_{off} is observed (Figure 8B). Finally, r also featured a strong upregulation as a function of average fluorescence across stripes (Figure 8C).

As shown in Figure 8D, each stripe contains nuclei with a relatively wide range of average fluorescence values. In order to reveal the bursting parameters across the AP axis for each stripe, we averaged the single-cell bursting parameters determined in each stripe (Figure 8A-C) weighted by the relative number of nuclei in each fluorescence bin present at each position along the AP axis (Figure 8D). We find that the variation in bursting parameters observed as a function of average fluorescence largely echoes the modulation of fluorescence in space (Figure 8E). Specifically, while there is a subtle downregulation of k_{off} within stripes, k_{on} and r are significantly upregulated in the center of each stripe.

Thus, not only do the five *eve* enhancers employ a common regulatory strategy for modulating the fluorescence output of nuclei to create a stripe, decreasing burst separation and increasing burst amplitude with a constant burst duration, the precise quantitative relationship among these bursting parameters is maintained across a wide range of molecular inputs and fluorescence outputs.

Discussion

The most remarkable aspect of *eve* regulation is that what appears to be a regular, repeating pattern of nearly identical stripes is created by the largely independent activity of five separate enhancers responding to different combinations of activators and repressors (Fujioka et al. 1999; Fujioka, Jaynes, and Goto 1995; Small et al. 1991; Arnosti et al. 1996; Small, Blair, and Levine 1992). We have now shown that the connection between the stripe enhancers is more than just that they produce the same kind of pattern: they realize these patterns through the same control of transcriptional bursting.

Although, in principle, complex patterns of transcription could be generated by the independent regulation of k_{on}, k_{off} or r, many of the key features of *eve* stripe regulation we observe here involve the modulation of k_{on} and r in concert. The most straightforward explanation for this shared mode of bursting control is that there is a single molecular pathway via which *eve* transcriptional bursting is regulated, with enhancers essentially having access to only a single tunable parameter. Whether this parameter is determined by the gene through, for example, the promoter sequence, or whether this single molecular pathway reflects some broad common property of gene regulation, such as constraints on the general transcriptional machinery, remains an open question. The limited data on bursting control available for other genes in the fly (Falo-Sanjuan et al., n.d.; Fukaya, Lim, and Levine 2016; Zoller, Little, and Gregor 2018) suggests that control mechanisms are not ubiquitously the same and that they might be unique to different classes of genes.

An alternative explanation for the observed commonalities in the control of bursting is that there is a functional reason to use this strategy. Namely, that this is not the result of a common molecular mechanism, but rather of common selective pressures acting on the five enhancers independently. The particular bursting control strategy uncovered here might, for example, be more robust to fluctuations in transcription factor concentrations or temperature, or provide more precise spatiotemporal gene expression control (Shelansky and Boeger 2020; Grah, Zoller, and Tkačik, n.d.). New experiments and theoretical work will be necessary in order to uncover the specific molecular pathways by which bursting is controlled and to understand the functional consequences of different bursting strategies that create the same mRNA levels.

In addition to this modulation of bursting, the fraction of nuclei that engage in transcription at any point in the nuclear cycle is higher in stripe centers than in interstripes. This regulation of the fraction of active nuclei, also seen in other genes (Garcia et al. 2013), seems to reside outside of the bursting framework. Such regulation, as well as the spatial modulation of the

window of time over which bursting ensues, suggests the presence of multiple and overlapping modes of regulation that go beyond the control of bursting parameters and that can be as relevant for pattern formation (Lammers et al. 2020).

Stripe movement is driven primarily by expression flow

Just as gene expression patterns are dynamic in time (J. P. Bothma et al. 2014), they are dynamic in space, resulting in the movement of expression domains throughout the embryo during development (Jaeger, Surkova, et al. 2004; Keränen et al. 2006). The anterior movement of *eve* stripes during nc14 has been previously described (Keränen et al. 2006; Lim et al. 2018), and proposed to arise from a combination of nuclear movement (nuclear flow) and movement in the pattern of regulators (expression flow), especially repressors, which are known to shift anteriorly during nc14 as well (Jaeger, Surkova, et al. 2004; Jaeger, Blagov, et al. 2004). While Keränen *et al.* (Keränen et al. 2006) concluded that the relative contributions of these two forces were roughly equal, our data suggest that, especially in the posterior, expression flow dominates the anterior shift of the *eve* stripes.

A typical nucleus in stripe 7 moves around one percent of embryo length in the final 25 min of nc14. The stripe, however, moves around five percent of embryo length during that time (see Figure 7C). Because we are tracking both the position and activity of individual nuclei, we can visualize expression flow in action. We see nuclei transition from low activity in the anterior interstripe to high activity in the stripe, from high activity in the stripe to low activity off the posterior flank of *eve* expression, and in some cases both.

This effect is most pronounced for the posterior stripes, but is observed for the more anterior stripes as well, although the magnitude of the shift decreases for more anterior stripes (Figure 7-S1). The difference in the amount of the effect we and Keränen *et al.* attribute to expression flow is likely an effect of differences in the data used. Because we are looking at instantaneous transcription rates while they looked at accumulated mRNA, there is a considerable temporal lag and integration of the transcriptional activity over the life time of *eve* mRNA in their data, which has the effect of underestimating the extent to which the stripes actually move.

We also note that the extent to which nuclear flow by itself would be expected to shift output patterns measured as a function of position in the embryo is unclear, as it would depend on the extent to which the repositioning of regulators drives movement of nuclei (which it is believed to

do (Blankenship and Wieschaus 2001)), and the corresponding effect that nuclear movement has on the positioning of regulators, which remains largely unknown.

One open question relates to the temporal relationship between changes in the position of the repressor array that drives stripe position and the transcriptional output of the stripes. For example, the anterior shift of the stripes of *eve* as well as *fushi tarazu* has been proposed to originate, in part, from cross-repression between these two genes (Lim et al. 2018). Recent advances in the simultaneous monitoring of protein concentration and transcriptional output in living embryos should help answer this question in the near future (J. P. Bothma et al. 2018; Lammers et al. 2020).

Characterizing dynamics patterns demands dynamics measurements

That gene expression is a fundamentally dynamic process is not new information. However, the tools we have had at our disposal to study gene expression so far have tended to emphasize its static features, down to the language we use to describe the transcriptional output of a gene. In textbooks and the scientific literature, *eve* has a gene expression pattern consisting of seven stripes. But, as some earlier work emphasized (Janssens et al. 2006), and we have directly visualized here, the transcriptional output of *eve*, rather than a single “pattern” is a rapidly changing as a function of time and space: it is dynamic at many time scales and across space and nuclear positions. Indeed, at no point does *eve* approach anything even remotely like a steady state.

We are at the dawn of a new period in the study of transcription, as new experimental techniques and advanced microscopy allow us to monitor transcriptional regulators, observe their behavior at the single-molecule level, and track the transcriptional output of a gene in living, developing animals. We have only barely begun to understand this new data and what it can tell us about biology. While the focus in this paper was on a single gene in a single species, we hope that this and our accompanying work (Lammers et al. 2020) will have a broader impact by beginning to establish rigorous frameworks for quantifying, characterizing and visualizing the dynamics of transcription at the single-cell level during development that will be required in the era of live imaging of transcription in development.

Methods

Generation of MS2 tagged *eve* BAC

We used bacterial recombineering (Warming et al. 2005) to modify a bacterial artificial chromosome (BAC) (Venken et al. 2006) containing the *D. melanogaster eve* gene and all of its enhancers and regulatory elements (BAC CH322-103K22) (Venken et al. 2009). We replaced the coding region with an array of 24 MS2 stem loops fused to the *D. melanogaster yellow* gene (Figure 1B; (J. P. Bothma et al. 2014) as described below. We inserted our eve::MS2::yellow BAC-based construct in the *D. melanogaster* genome at chromosome 3L through ΦC31 integrase-mediated recombination (see Generation of fly lines), and generated a viable homozygous fly line (w-; +; eve::MS2::yellow) as detailed below.

Reporter design

In principle the length of the reporter should not limit our ability to estimate burst parameters. However, in practice a reporter construct that is too short will have insufficient signal. Further, one that is too long will increase the dwell time of each RNA polymerase molecule on the gene and, as a result, our cpHMM inference will require too many computational resources. Our choice of reporter construct structure strikes a balance between these two limitations and is ideally suited for inferring bursting parameters in the time range where eve resides, as well as for boosting the signal-to-noise ratio. See Lammers *et al.* (2020) for a more detailed discussion of reporter length-related tradeoffs.

Specifics of recombineering

We modified a CHORI BAC CH322-103K22 derived from (Venken et al. 2009), which contained the entire *eve* locus and a GFP reporter instead of the *eve* coding sequence (CH322-103K22-GFP). We replaced the GFP reporter with MS2::*yellow* (6665 bp) through a two step, scarless, *galK* cassette-mediated bacterial recombineering (Warming et al. 2005). Briefly, we transformed our starting CH322-103K22-GFP BAC into *E.coli* recombineering strain SW102. We then electroporated the strain with a *galK* cassette flanked by 50bp-long DNA homology arms homologous to the MS2::*yellow* (6665 bp) reporter. Upon electroporation, we selected transformants on M63 minimal media plates with galactose as a single carbon source. We achieved a correct replacement of GFP sequence by *galK* cassette in the BAC context

(CH322-103K22-galK), validated by observing the digestion patterns produced by ApaLI restriction enzyme.

We next purified the CH322-103K22-galK BAC and transformed it into fresh *E. coli* SW102 cells. We electroporated these cells with the purified MS2::*yellow* insert and used M63 minimal media plates with 2-deoxy-galactose to select against bacteria with a functional *galK* gene. We used colony PCR to screen for colonies with a correct MS2::*yellow* insertion (CH322-103K22-MS2) replacing the *galK* cassette. We validated this insertion by observing ApaLI, XhoI, SmaI, and EcoRI restriction digestion patterns and through PCR and Sanger sequencing of the insertion junctions. We transformed our CH322-103K22-MS2 BAC in *E.coli* EPI300 cells to induce high copy numbers and purified it with a Qiagen plasmid Midiprep kit.

Generation of fly lines

We sent a sample of our purified CH322-103K22-MS2 BAC to Rainbow Transgenic Flies, Inc. for injection in *D. melanogaster* embryos bearing a ΦC31 AttP insertion site in chromosome 3L (Bloomington stock #24871; landing site VK00033; cytological location 65B2). We received the flies that resulted from that injection and used a balancer fly line (w- ; + ; +/TM3sb) to obtain a viable MS2 homozygous line (w- ; + ; MS2::*yellow*). We used line (yw; His::RFP; MCP::GFP) as the maternal source of Histone-RFP and MCP-GFP (Garcia et al. 2013).

Embryo Collection and Mounting

Embryo collection and mounting was done as specified in (Garcia and Gregor 2018). In short, we set fly crosses between ~30 males (w-; +; eve::MS2::yellow) and ~80 females (yw; His::RFP; MCP::GFP) in a plastic cage capped with a grape juice agar plate. We collected embryos from cages two to ten days old by adding a fresh plate for 30 minutes and aging for 60 minutes to target embryos 90 min or younger.

Embryos were mounted on a gas-permeable Lumox Film (Sarstedt - Catalog # 94.6077.317) embedded on a microscope slide hollowed on the center. Then, we coated the hydrophobic side of the Lumox film with heptane glue and let it dry. The film allows oxygenation of embryos during the 2-3h long imaging sessions while heptane immobilizes them.

We soaked an agar plate with Halocarbon 27 oil, picked embryos with forceps, and laid them down on a 3 x 3 cm piece of paper tissue. We dechorionated embryos by adding 2 drops of bleach diluted in water (5.25%) on the paper tissue and incubating for 1.5 minute. We removed bleach with a clean tissue and rinsed with ~4 drops of distilled water. We then placed

the tissue paper with dechorionated embryos in water, and picked buoyant embryos with a brush.

We lined ~30 apparently healthy embryos on the Lumox film slide and added 2-3 drops of Halocarbon 27 oil to avoid desiccation, and covered the embryos with a cover slip (Corning® Cover Glass, No.1, 18 x 18mm) for live imaging.

Imaging and Optimization of Data Collection

Movies of embryonic development were recorded on a Zeiss-800 confocal laser scanning microscope in two channels, (EGFP: 488 nm; TagRFP: 561 nm). We imaged embryos on a wide field of view, along their anterior-posterior axis, of 1024 x 256 pixels (202.8μm x 50.7μm), encompassing 3-5 stripes per movie. We tuned laser power, scanning parameters, master gain, pinhole size and laser power to optimize signal to noise ratio without significant photobleaching and phototoxicity.

For imaging, the following microscope settings were used: 63x oil-objective, scan mode 'frame', pixel size of 0.2μm, 16 bits per pixel, bidirectional scanning at a speed of 7, line step of 1, laser scanner dwelling per pixel of 1.03μs, laser scanner averaging of 2, averaging method Mean, averaging mode Line, 488 nm laser power of 30μW (EGFP), 561 nm laser power of 7.5μW (TagRFP) (both powers were measured with a 10x air-objective), Master Gain in EGFP detector of 550V, Master Gain in TagRFP detector of 650V, Digital Offset in both detectors of 0, Digital Gain in both detectors of 1.0, and a pinhole size of 1 airy unit under the imaging conditions mentioned above (44μm, 0.7μm/section), laser filters EGFP:SP545 and TagRFP:LBF640. This resulted in an imaging time of 633 ms per frame and a full Z-stack of 21 frames in intervals of 0.5μm every 16.8s. Following (J. P. Bothma et al. 2014, 2015, 2018; Lammers et al. 2020), the imaging conditions were determined not to affect normal development as reported by the timing of the nuclear cycles in early development. We stopped imaging after 50 min into nuclear cycle 14, and took mid-sagittal and surface pictures of the whole embryo for localization of the recorded field of view along the embryo's AP axis.

Image processing

We used a Matlab computational pipeline based on (Garcia et al. 2013; Lammers et al. 2020) to segment and extract numeric data from our raw movies. Briefly, this software segments and processes the images from the two channels (channel 1: MCP::GFP, channel 2: Histone::RFP) on which we collected our data. For segmentation of channel 1, we used

Fiji-Weka Segmentation 3D software; this machine-learning-based method relies on the manual segmentation of a variety of MCP::GFP labeled transcriptional foci in a given 21 frame Z-stack from a single dataset (EVE_D11) to produce a model for the segmentation of all datasets recorded under the same imaging conditions. Next, we segmented and tracked the Histone::RFP labeled nuclei on channel 2. Subsequently, we assigned MCP::GFP labeled transcriptional foci to their corresponding Histone::RFP labeled nuclei. Since we collected whole embryo pictures of each of our datasets, we were able to match and locate the recorded fields of view to their right position along the body of their corresponding embryos. Finally, we extracted position and fluorescence values over time of all transcriptional foci to generate data structures ready to use in further analyses.

Estimation of polymerase transit time

To estimate the transit time of the polymerase along the construct (which is used to determine the persistence of the fluorescence signal from a single transcript at the locus) we first calculated, for each nucleus, the difference in fluorescence signal between adjacent timepoints $D_{n,t} = F_{n,t+1} - F_{n,t}$ where $F_{n,t}$ is the fluorescence signal for nucleus *n* at time point *t* and then calculated the Pearson correlation coefficient of the vectors [..., $D_{n,t}$, $D_{n,t+1}$, $D_{n,t+2}$, ...] and [..., $D_{n,t+d}$, $Dn,_{t+d+1}$, $D_{n,t+d+2}$, ...] over values of d from 1 to 20 representing time displacements of 20 to 400 seconds. The minimum correlation occurred at 140 seconds.

Compound-state Hidden Markov Model

For this work we employed a statistical method that utilizes a compound-state Hidden Markov Model to infer bursting parameters from experimental fluorescence traces. The theory and implementation of this method are described in detail in (Lammers et al. 2020). Briefly, parameters were inferred using a standard version of the Expectation Maximization Algorithm implemented using custom-written scripts in Matlab. Our inference is carried over the full duration of activity of each active nucleus during nuclear cycle 14. Bootstrap sampling was used to estimate the standard error in our parameter estimates. Subsets of 3,000 data points were used to generate time-averaged parameter estimates. Inference was not conducted for groups for which fewer than 1,000 time points were available.

Data Analysis and Figures

All data were analyzed in Python using a Jupyter notebook with custom code to process raw data and generate figures. The Jupyter notebook and all data required to run it is available in File S1.

Data Filtering

We first filtered the raw data to remove data with observations spanning less than 2,000 seconds, as well as nuclei that were poorly tracked over time (defined as nuclei that moved across the movies at an average rate of over 4.5 pixels per minute. This left 430,073 observations from 2,959 nuclei.

Stripe assignment and registration

We used the Gaussian mixture model module of the Python library scikit-learn (Pedregosa et al. 2011) to cluster all nuclei time points in each movie in each of a series of overlapping 428 second time windows beginning at 25 min in nc14, specifying the number of components equal to the number of stripes captured in the movie and using the setting *covariance_type='tied'.* We preliminarily assigned nuclei time points to a stripe if they were consistently clustered in that stripe in the relevant time windows. We then pooled all nuclei time points assigned to the same stripe and fit a line to the median x and y positions in the bottom ($y < 128$) and top ($y > 128$) halves of the image. We considered the slope of this line to represent the orientation of the stripe to the image x axis. We then went back to each time window and fit the nuclei assigned to the stripe with a line with the previously computed slope fixed. This produced an association of time with stripe position, from which we derived a linear model that describes the position of each stripe in each movie at every time point.

We assigned all nuclei time points (not just bursting ones) to stripes by identifying the stripe whose predicted position at the relevant time was closest (along the x axis) to the nucleus being analyzed, and assigned a nucleus to the most common stripe assignment for its individual time points. We then corrected the reorientation of the stripe at each time point to be perpendicular to the image x-axis (to enable projection along the AP axis) by setting its new image x-axis position to be the x position of the stripe in the middle of the y-axis ($y = 128$) plus the offset of the nucleus to the unoriented stripe along the x-axis. Finally, we used the positions of the anterior and posterior poles of the embryo to map image x coordinates to AP position. We then adjusted the AP position of each stripe in each movie such that the center of the stripe at 35 min in nc14 had the same AP position.

Author contributions

AB designed and generated the labeled *eve* transgene, collected all of the imaging data and ran the initial image processing. NL and MBE performed all of the higher level analyses and generated figures. HGG and MBE wrote the paper. HGG and MBE conceived of the experiments. HGG and MBE provided funding and supervised every aspect of the project.

Data Availability

All of the raw and processed data described in this paper as well as links to code and computational notebooks are available in File S1 and at http://www.eisenlab.org/eve7.

Acknowledgements

This work was supported by an HHMI Investigator award to MBE. HGG was supported by the Burroughs Wellcome Fund Career Award at the Scientific Interface, the Sloan Research Foundation, the Human Frontiers Science Program, the Searle Scholars Program, the Shurl & Kay Curci Foundation, the Hellman Foundation, the NIH Director's New Innovator Award (DP2 OD024541-01), and an NSF CAREER Award (1652236). NL was supported by NIH Genomics and Computational Biology training grant 5T32HG000047-18. AB was supported by a Doctoral Fellowship from The University of California Institute for Mexico and the United States (UC MEXUS) and CONACyT.

Figure captions:

Figure 1. Visualizing live transcription from the seven stripes of *D. melanogaster even-skipped*. (A) Simple model of transcriptional bursting by promoter switching between ON and OFF states. (B) The promoter switching parameters define the burst duration, the duration between bursts, and amplitude. (C) Wild-type *eve* locus showing the five stripe enhancers (1,2,3+7,4+6,5) and the late enhancer element. Colors for individual stripes are used throughout figures. (D) Layout of the engineered *eve* BAC showing the locations of the MS2 stem loop array and *yellow* gene.

Figure 2. Live expression of *even-skipped.* Stills from maximum projection renderings of image stacks of an embryo spanning all seven stripes. This movie was collected with a 40x objective for illustration purposes only. Movies used for data analysis were collected at higher resolution as described in the text.

Figure 3. Spatiotemporal dynamics of *even-skipped* expression. (A) Fluorescence traces from two representative nuclei (particle ID = 1.0163 and 11.0448). (B) Average fluorescence over space and time showing stripe formation, modulation and movement. The time resolution along the y-axis is 20s. The positions of nuclei along the x-axis were registered across movies based on the inferred position of stripe centers, and placed into bins of one percent embryo length, with the average fluorescence of all nuclei in each bin plotted. (A, shading corresponds to the error estimated based on the background fluorescence fluctuations as described in (Garcia et al. 2013)).

Figure 4. Modeling bursting in individual nuclei. (A) A key parameter in relating fluorescence output to the bursting state of a promoter is the time it takes for a polymerase to transit the gene, which we determined as approximately 140s by examining the autocorrelation (red line) of the change in fluorescence. Gray lines show 100 bootstraps over randomly selected sets of 80% of nuclei; note they almost perfectly overlap the red line. (B) Three state model accounting for post-replication presence of sister chromatids. When either promoter is ON for a short time period Δt, loads polymerases at a constant rate contributing a pulse of polymerase that persists for 140s. (C) Simplified example of the expected observed fluorescence (red line) produced from a hypothetical promoter state sequence. The fluorescence is the sum of the fluorescence pulses produced when one or both promoters are ON (given by the height of the green bars). (D-F) Representative fluorescence traces from individual nuclei (blue lines), inferred bursting pattern (green bars) and fluorescence imputed by cpHMM (red line) for particles 1.0163 (D), 11.0448 (E) and 5.0231 (F).

Figure 5. Stripe assignment and alignment. (A) We preliminarily assign bursting nuclei to stripes by applying a Gaussian mixture model to each movie independently in overlapping six-minute time windows with the number of Gaussians equal to the number of stripes captured in that movie. An example is shown here from Movie 2. (B,C,D) We next determine the orientation of each stripe to the imaging axes by fitting a line to coordinates of all nuclei from t > 25 min assigned to that stripe in each movie and time window. (E) We use these fits to generate a linear model of the position of each stripe in each image over time, which makes it possible to reorient the stripe so that it is perpendicular to the image x-axis . (F) The known coordinates of the anterior and posterior poles of the embryo are used to convert the image x-axis to AP position and register the stripes from different movies to each other, as shown here for nuclei from Movie 2 colored by stripe and nuclei corresponding to all other movies drawn in grey.

Figure 6. The kinetic fingerprint of *even-skipped* stripe formation. (A) Inferred location of every transcriptional burst in all 11 movies as a function of time and where along the anterio-posterior axis (plotted as fraction of embryo length) each burst occurred. The size of the dot represents the duration of the burst. Collectively the data create a kinetic fingerprint of *eve* stripe formation. (B) Instantaneous fraction of nuclei in the transcriptionally active ON state as a function of time and position along the embryo.

Figure 7. Stripe formation and movement. (A) Fraction of nuclei bursting before time *t* as a function of position along the embryo. (B) Locations of new bursts (black dots) in space and time along with spatiotemporal traces of nuclei that are in the OFF state throughout nc14 (red lines). (C) Traces of nuclei positions over time (gray lines) from stripe 7 region of movie EVE_D6 with timepoints where new bursts initiated colored red to illustrate stripe movement relative to nuclei. (D) Difference in transcriptional activity as defined as the difference between the fraction of the time each nucleus is in the ON state in the subsequent 10 min minus the fraction of time the nucleus is in the ON state in the preceding 10 min. Positive values represent a nucleus turning on or increasing activity, while blue values indicate a nucleus turning off or decreasing activity.

Figure 7-S1. Stripe movement is dominated by the movement of transcriptional activity. Traces of nuclei positions over time (gray lines) from all eleven movies with time points corresponding to transcriptional bursts annotated as in stripes colored red.

Figure 8. A common bursting control mechanism across all *even-skipped* stripes. (A-C) cpHMM inference was carried over nuclei binned according to their average fluorescence value indicating that while (A) k_{on} and (C) r are subject to the same regulation along all stripes, (B) k_{off} remains unchanged. Error bars are calculated by

taking the standard deviation across cpHMM inference results for multiple bootstrapped samples of experimental data. (D) Distribution of average nuclear fluorescence values along the AP axis. (E) Mean nuclear fluorescence values for each AP position together with the corresponding averaged and weighted bursting parameters.

Tables

Table 1. Summary of movies collected.

Embryo ID	Duration	Stripes	Data Movies	Promoter State Movies
EVE_D1	255 frames 71.2 min	1-4	Video 2	Video 13
EVE_D2	254 frames 70.9 min	3-7	Video 3	Video 14
EVE_D3	235 frames 65.6 min	3-6	Video 4	Video 15
EVE_D4	246 frames 68.7 min	3-7	Video 5	Video 16
EVE_D5	210 frames 58.6 min	4-7	Video 6	Video 17
EVE_D6	196 frames 54.7 min	4-7	Video 7	Video 18
EVE_D7	208 frames 58.1 min	3-7	Video 8	Video 19
EVE_D8	232 frames 64.8 min	1-3	Video 9	Video 20
EVE_D9	322 frames 89.9 min	1-4	Video 10	Video 21
EVE_D10	267 frames 74.5 min	1-3	Video 11	Video 22
EVE_D11	307 frames 85.7 min	1-4	Video 12	Video 23

All videos are available at https://www.dropbox.com/sh/74liy57g5kxmjwr/AADUzporIqPWFnuJkV6ERuYza?dl=0. All data videos 16.76 fps. Promoter state movies are at 20 fps.

Videos

All videos are available at
https://www.dropbox.com/sh/74liy57g5kxmjwr/AADUzporIqPWFnuJkV6ERuYza?dl=0

Video 1. Full expression pattern of *eve*-MS2 BAC. Maximum value projection of Z-stacks of an entire embryo carrying *eve*-MS2 BAC, MCP-GFP and histone-RFP imaged with a 40x objective.

Videos 2-12. Individual dataset movies. Maximum value projection of Z-stacks of sections of embryos carrying *eve*-MS2 BAC, MCP-GFP and histone-RFP imaged with a 63x objective, each capturing 3-5 stripes as described in Table 1.

Videos 13-23. Promoter state movies. Animation of pseudo-cells (resulting from a Voronoi tessellation based on the position of nuclei) where cells are colored based on their stripe, with intensity proportional to the measured *eve* MS2 fluorescence of the nucleus at the given time, and promoters in the ON and OFF states represented with light and dark gray pseudo-cell outlines, respectively.

Video 24. Kinetic fingerprint of *eve* stripe formation. Nuclei are graphed at every time point at its registered AP (x-axis) and image y (y-axis) position when the cpHMM inferred that one copy (small circles) or two copies (large circles) of the promoter was in the ON state (see Figure 4B).

References

Arnosti, D. N., S. Barolo, M. Levine, and S. Small. 1996. “The Eve Stripe 2 Enhancer Employs Multiple Modes of Transcriptional Synergy.” *Development* 122 (1): 205–14.

Bartman, Caroline R., Sarah C. Hsu, Chris C. -S. Hsiung, Arjun Raj, and Gerd A. Blobel. 2016. “Enhancer Regulation of Transcriptional Bursting Parameters Revealed by Forced Chromatin Looping.” *Molecular Cell* 62 (2): 237–47.

Bertrand, E., P. Chartrand, M. Schaefer, S. M. Shenoy, R. H. Singer, and R. M. Long. 1998. “Localization of ASH1 mRNA Particles in Living Yeast.” *Molecular Cell* 2 (4): 437–45.

Blake, William J., Gábor Balázsi, Michael A. Kohanski, Farren J. Isaacs, Kevin F. Murphy, Yina Kuang, Charles R. Cantor, David R. Walt, and James J. Collins. 2006. “Phenotypic Consequences of Promoter-Mediated Transcriptional Noise.” *Molecular Cell* 24 (6): 853–65.

Blankenship, J. T., and E. Wieschaus. 2001. “Two New Roles for the Drosophila AP Patterning System in Early Morphogenesis.” *Development* 128 (24): 5129–38.

Boettiger, Alistair Nicol, and Michael Levine. 2013. “Rapid Transcription Fosters Coordinate Snail Expression in the Drosophila Embryo.” *Cell Reports* 3 (1): 8–15.

Bothma, Jacques, and Michael Levine. 2013. “Development: Lights, Camera, Action — The Drosophila Embryo Goes Live!” *Current Biology: CB* 23 (21): R965–67.

Bothma, Jacques P., Hernan G. Garcia, Emilia Esposito, Gavin Schlissel, Thomas Gregor, and Michael Levine. 2014. “Dynamic Regulation of Eve Stripe 2 Expression Reveals Transcriptional Bursts in Living Drosophila Embryos.” *Proceedings of the National Academy of Sciences* 111 (29): 10598–603.

Bothma, Jacques P., Hernan G. Garcia, Samuel Ng, Michael W. Perry, Thomas Gregor, and Michael Levine. 2015. “Enhancer Additivity and Non-Additivity Are Determined by Enhancer Strength in the Drosophila Embryo.” *eLife* 4 (August). https://doi.org/10.7554/eLife.07956.

Bothma, Jacques P., Matthew R. Norstad, Simon Alamos, and Hernan G. Garcia. 2018. “LlamaTags: A Versatile Tool to Image Transcription Factor Dynamics in Live Embryos.” *Cell* 0 (0). https://doi.org/10.1016/j.cell.2018.03.069.

Choubey, Sandeep, Jane Kondev, and Alvaro Sanchez. 2015. “Deciphering Transcriptional Dynamics In Vivo by Counting Nascent RNA Molecules.” *PLoS Computational Biology* 11 (11): e1004345.

———. 2018. “Distribution of Initiation Times Reveals Mechanisms of Transcriptional Regulation in Single Cells.” *Biophysical Journal* 114 (9): 2072–82.

Chubb, Jonathan R., Tatjana Trcek, Shailesh M. Shenoy, and Robert H. Singer. 2006. “Transcriptional Pulsing of a Developmental Gene.” *Current Biology: CB* 16 (10): 1018–25.

Clyde, Dorothy E., Maria S. G. Corado, Xuelin Wu, Adam Paré, Dmitri Papatsenko, and Stephen Small. 2003. “A Self-Organizing System of Repressor Gradients Establishes Segmental Complexity in Drosophila.” *Nature* 426 (6968): 849–53.

Coulon, A., and D. R. Larson. 2016. “Fluctuation Analysis: Dissecting Transcriptional Kinetics with Signal Theory.” *Methods in Enzymology* 572 (April): 159–91.

Desponds, Jonathan, Huy Tran, Teresa Ferraro, Tanguy Lucas, Carmina Perez Romero, Aurelien Guillou, Cecile Fradin, Mathieu Coppey, Nathalie Dostatni, and Aleksandra M. Walczak. 2016. “Precision of Readout at the Hunchback Gene: Analyzing Short Transcription Time Traces in Living Fly Embryos.” *PLoS Computational Biology* 12 (12): e1005256.

Falo-Sanjuan, Julia, Nicholas C. Lammers, Hernan G. Garcia, and Sarah Bray. n.d. “Enhancer Priming Enables Fast and Sustained Transcriptional Responses to Notch Signaling.” https://doi.org/10.1101/497651.

Fish, Matthew P., Amy C. Groth, Michele P. Calos, and Roel Nusse. 2007. “Creating Transgenic Drosophila by Microinjecting the Site-Specific phiC31 Integrase mRNA and a Transgene-Containing Donor Plasmid.” *Nature Protocols* 2 (10): 2325–31.

Forrest, Kevin M., and Elizabeth R. Gavis. 2003. “Live Imaging of Endogenous RNA Reveals a Diffusion and Entrapment Mechanism for Nanos mRNA Localization in Drosophila.” *Current Biology: CB* 13 (14): 1159–68.

Fowlkes, Charless C., Cris L. Luengo Hendriks, Soile V. E. Keränen, Gunther H. Weber, Oliver Rübel, Min-Yu Huang, Sohail Chatoor, et al. 2008. “A Quantitative Spatiotemporal Atlas of Gene Expression in the Drosophila Blastoderm.” *Cell* 133 (2): 364–74.

Frasch, M., and M. Levine. 1987. “Complementary Patterns of Even-Skipped and Fushi Tarazu Expression Involve Their Differential Regulation by a Common Set of Segmentation Genes in Drosophila.” *Genes & Development* 1 (9): 981–95.

Fujioka, M., Y. Emi-Sarker, G. L. Yusibova, T. Goto, and J. B. Jaynes. 1999. “Analysis of an Even-Skipped Rescue Transgene Reveals Both Composite and Discrete Neuronal and Early Blastoderm Enhancers, and Multi-Stripe Positioning by Gap Gene Repressor Gradients.” *Development* 126 (11): 2527–38.

Fujioka, M., J. B. Jaynes, and T. Goto. 1995. “Early Even-Skipped Stripes Act as Morphogenetic Gradients at the Single Cell Level to Establish Engrailed Expression.” *Development* 121 (12): 4371–82.

Fukaya, Takashi, Bomyi Lim, and Michael Levine. 2016. “Enhancer Control of Transcriptional Bursting.” *Cell* 166 (2): 358–68.

———. 2017. “Rapid Rates of Pol II Elongation in the Drosophila Embryo.” *Current Biology: CB* 27 (9): 1387–91.

Fung, Jennifer C., Wallace F. Marshall, Abby Dernburg, David A. Agard, and John W. Sedat. 1998. “Homologous Chromosome Pairing inDrosophila melanogasterProceeds through Multiple Independent Initiations.” *The Journal of Cell Biology* 141 (1): 5–20.

Garcia, Hernan G., Augusto Berrocal, Yang Joon Kim, Gabriella Martini, and Jiaxi Zhao. 2020. “Lighting up the Central Dogma for Predictive Developmental Biology.” *Current Topics in Developmental Biology*. https://doi.org/10.1016/bs.ctdb.2019.10.010.

Garcia, Hernan G., and Thomas Gregor. 2018. “Live Imaging of mRNA Synthesis in Drosophila.” *Methods in Molecular Biology* 1649: 349–57.

Garcia, Hernan G., Mikhail Tikhonov, Albert Lin, and Thomas Gregor. 2013. “Quantitative Imaging of Transcription in Living Drosophila Embryos Links Polymerase Activity to Patterning.” *Current Biology: CB* 23 (21): 2140–45.

Golding, Ido, Johan Paulsson, Scott M. Zawilski, and Edward C. Cox. 2005. “Real-Time Kinetics of Gene Activity in Individual Bacteria.” *Cell* 123 (6): 1025–36.

Goto, Tadaatsu, Paul Macdonald, and Tom Maniatis. 1989. “Early and Late Periodic Patterns of Even Skipped Expression Are Controlled by Distinct Regulatory Elements That Respond to Different Spatial Cues.” *Cell* 57 (3): 413–22.

Grah, Rok, Benjamin Zoller, and Gašper Tkačik. n.d. “Normative Models of Enhancer Function.” https://doi.org/10.1101/2020.04.08.029405.

Harding, K., T. Hoey, R. Warrior, and M. Levine. 1989. “Autoregulatory and Gap Gene Response Elements of the Even-Skipped Promoter of Drosophila.” *The EMBO Journal* 8 (4): 1205–12.

Hendy, Oliver, John Campbell Jr, Jocelyn D. Weissman, Daniel R. Larson, and Dinah S. Singer. 2017a. “Differential Context-Specific Impact of Individual Core Promoter Elements on Transcriptional Dynamics.” *Molecular Biology of the Cell* 28 (23): 3360–70.

———. 2017b. “Differential Context-Specific Impact of Individual Core Promoter Elements on

Transcriptional Dynamics." *Molecular Biology of the Cell* 28 (23): 3360–70.
Holloway, David M., and Alexander V. Spirov. 2017. "Transcriptional Bursting in Drosophila Development: Stochastic Dynamics of Eve Stripe 2 Expression." *PloS One* 12 (4): e0176228.
Jaeger, Johannes, Maxim Blagov, David Kosman, Konstantin N. Kozlov, Manu, Ekaterina Myasnikova, Svetlana Surkova, et al. 2004. "Dynamical Analysis of Regulatory Interactions in the Gap Gene System of Drosophila Melanogaster." *Genetics* 167 (4): 1721–37.
Jaeger, Johannes, Svetlana Surkova, Maxim Blagov, Hilde Janssens, David Kosman, Konstantin N. Kozlov, Manu, et al. 2004. "Dynamic Control of Positional Information in the Early Drosophila Embryo." *Nature* 430 (6997): 368–71.
Janicki, Susan M., Toshiro Tsukamoto, Simone E. Salghetti, William P. Tansey, Ravi Sachidanandam, Kannanganattu V. Prasanth, Thomas Ried, et al. 2004. "From Silencing to Gene Expression: Real-Time Analysis in Single Cells." *Cell* 116 (5): 683–98.
Janssens, Hilde, Shuling Hou, Johannes Jaeger, Ah-Ram Kim, Ekaterina Myasnikova, David Sharp, and John Reinitz. 2006. "Quantitative and Predictive Model of Transcriptional Control of the Drosophila Melanogaster Even Skipped Gene." *Nature Genetics* 38 (10): 1159–65.
Jiang, Pengyao, Michael Z. Ludwig, Martin Kreitman, and John Reinitz. 2015. "Natural Variation of the Expression Pattern of the Segmentation Gene Even-Skipped in Melanogaster." *Developmental Biology* 405 (1): 173–81.
Jones, Daniel L., Robert C. Brewster, and Rob Phillips. 2014. "Promoter Architecture Dictates Cell-to-Cell Variability in Gene Expression." *Science* 346 (6216): 1533–36.
Kepler, Thomas B., and Timothy C. Elston. 2001. "Stochasticity in Transcriptional Regulation: Origins, Consequences, and Mathematical Representations." *Biophysical Journal* 81 (6): 3116–36.
Keränen, Soile V. E., Charless C. Fowlkes, Cris L. Luengo Hendriks, Damir Sudar, David W. Knowles, Jitendra Malik, and Mark D. Biggin. 2006. "Three-Dimensional Morphology and Gene Expression in the Drosophila Blastoderm at Cellular Resolution II: Dynamics." *Genome Biology* 7 (12): R124.
Ko, Minoru S. H. 1991. "A Stochastic Model for Gene Induction." *Journal of Theoretical Biology* 153 (2): 181–94.
Lammers, Nicholas C., Vahe Galstyan, Armando Reimer, Sean A. Medin, Chris H. Wiggins, and Hernan G. Garcia. 2020. "Multimodal Transcriptional Control of Pattern Formation in Embryonic Development." *Proceedings of the National Academy of Sciences of the United States of America* 117 (2): 836–47.
Lawrence, Peter A. 1992. *The Making of a Fly: The Genetics of Animal Design*. 1 edition. Wiley-Blackwell.
Lenstra, Tineke L., Antoine Coulon, Carson C. Chow, and Daniel R. Larson. 2015. "Single-Molecule Imaging Reveals a Switch between Spurious and Functional ncRNA Transcription." *Molecular Cell* 60 (4): 597–610.
Lim, Bomyi, Takashi Fukaya, Tyler Heist, and Michael Levine. 2018. "Temporal Dynamics of Pair-Rule Stripes in Living Embryos." *Proceedings of the National Academy of Sciences of the United States of America* 115 (33): 8376–81.
Lionnet, Timothée, Kevin Czaplinski, Xavier Darzacq, Yaron Shav-Tal, Amber L. Wells, Jeffrey A. Chao, Hye Yoon Park, Valeria de Turris, Melissa Lopez-Jones, and Robert H. Singer. 2011. "A Transgenic Mouse for in Vivo Detection of Endogenous Labeled mRNA." *Nature Methods* 8 (2): 165–70.
Little, Shawn C., Mikhail Tikhonov, and Thomas Gregor. 2013. "Precise Developmental Gene

Expression Arises from Globally Stochastic Transcriptional Activity." *Cell* 154 (4): 789–800.
Ludwig, Michael Z., Manu, Ralf Kittler, Kevin P. White, and Martin Kreitman. 2011. "Consequences of Eukaryotic Enhancer Architecture for Gene Expression Dynamics, Development, and Fitness." *PLoS Genetics* 7 (11): e1002364.
Luengo Hendriks, Cris L., Soile V. E. Keränen, Charless C. Fowlkes, Lisa Simirenko, Gunther H. Weber, Angela H. DePace, Clara Henriquez, et al. 2006. "Three-Dimensional Morphology and Gene Expression in the Drosophila Blastoderm at Cellular Resolution I: Data Acquisition Pipeline." *Genome Biology* 7 (12): R123.
Macdonald, P. M., P. Ingham, and G. Struhl. 1986. "Isolation, Structure, and Expression of Even-Skipped: A Second Pair-Rule Gene of Drosophila Containing a Homeo Box." *Cell* 47 (5): 721–34.
Mannervik, Mattias. 2014. "Control of Drosophila Embryo Patterning by Transcriptional Co-Regulators." *Experimental Cell Research* 321 (1): 47–57.
McKnight, S. L., and O. L. Miller Jr. 1977. "Electron Microscopic Analysis of Chromatin Replication in the Cellular Blastoderm Drosophila Melanogaster Embryo." *Cell* 12 (3): 795–804.
Molina, N., D. M. Suter, R. Cannavo, B. Zoller, I. Gotic, and F. Naef. 2013. "Stimulus-Induced Modulation of Transcriptional Bursting in a Single Mammalian Gene." *Proceedings of the National Academy of Sciences* 110 (51): 20563–68.
Muramoto, Tetsuya, Danielle Cannon, Marek Gierlinski, Adam Corrigan, Geoffrey J. Barton, and Jonathan R. Chubb. 2012. "Live Imaging of Nascent RNA Dynamics Reveals Distinct Types of Transcriptional Pulse Regulation." *Proceedings of the National Academy of Sciences of the United States of America* 109 (19): 7350–55.
Padovan-Merhar, Olivia, Gautham P. Nair, Andrew G. Biaesch, Andreas Mayer, Steven Scarfone, Shawn W. Foley, Angela R. Wu, L. Stirling Churchman, Abhyudai Singh, and Arjun Raj. 2015. "Single Mammalian Cells Compensate for Differences in Cellular Volume and DNA Copy Number through Independent Global Transcriptional Mechanisms." *Molecular Cell* 58 (2): 339–52.
Paré, Adam, Derek Lemons, Dave Kosman, William Beaver, Yoav Freund, and William McGinnis. 2009. "Visualization of Individual Scr mRNAs during Drosophila Embryogenesis Yields Evidence for Transcriptional Bursting." *Current Biology: CB* 19 (23): 2037–42.
Peccoud, J., and B. Ycart. 1995. "Markovian Modeling of Gene-Product Synthesis." *Theoretical Population Biology* 48 (2): 222–34.
Pedregosa, Fabian, Gaël Varoquaux, Alexandre Gramfort, Vincent Michel, Bertrand Thirion, Olivier Grisel, Mathieu Blondel, et al. 2011. "Scikit-Learn: Machine Learning in Python." *Journal of Machine Learning Research: JMLR* 12 (Oct): 2825–30.
Rabinowitz, Morris. 1941. "Studies on the Cytology and Early Embryology of the Egg of Drosophila Melanogaster." *Journal of Morphology* 69 (1): 1–49.
Raj, Arjun, Charles S. Peskin, Daniel Tranchina, Diana Y. Vargas, and Sanjay Tyagi. 2006. "Stochastic mRNA Synthesis in Mammalian Cells." *PLoS Biology* 4 (10): e309.
Sanchez, Alvaro, Hernan G. Garcia, Daniel Jones, Rob Phillips, and Jané Kondev. 2011. "Effect of Promoter Architecture on the Cell-to-Cell Variability in Gene Expression." *PLoS Computational Biology* 7 (3): e1001100.
Sánchez, Álvaro, and Jané Kondev. 2008. "Transcriptional Control of Noise in Gene Expression." *Proceedings of the National Academy of Sciences* 105 (13): 5081–86.
Sasai, Masaki, and Peter G. Wolynes. 2003. "Stochastic Gene Expression as a Many-Body Problem." *Proceedings of the National Academy of Sciences of the United States of America* 100 (5): 2374–79.

Senecal, Adrien, Brian Munsky, Florence Proux, Nathalie Ly, Floriane E. Braye, Christophe Zimmer, Florian Mueller, and Xavier Darzacq. 2014. “Transcription Factors Modulate c-Fos Transcriptional Bursts.” *Cell Reports* 8 (1): 75–83.

Shahrezaei, V., and P. S. Swain. 2008. “Analytical Distributions for Stochastic Gene Expression.” *Proceedings of the National Academy of Sciences* 105 (45): 17256–61.

Shelansky, Robert, and Hinrich Boeger. 2020. “Nucleosomal Proofreading of Activator–promoter Interactions.” *Proceedings of the National Academy of Sciences*. https://doi.org/10.1073/pnas.1911188117.

Shermoen, Antony W., Mark L. McCleland, and Patrick H. O’Farrell. 2010. “Developmental Control of Late Replication and S Phase Length.” *Current Biology: CB* 20 (23): 2067–77.

Small, S., A. Blair, and M. Levine. 1992. “Regulation of Even-Skipped Stripe 2 in the Drosophila Embryo.” *The EMBO Journal* 11 (11): 4047–57.

Small, S., R. Kraut, T. Hoey, R. Warrior, and M. Levine. 1991. “Transcriptional Regulation of a Pair-Rule Stripe in Drosophila.” *Genes & Development* 5 (5): 827–39.

So, Lok-Hang, Anandamohan Ghosh, Chenghang Zong, Leonardo A. Sepúlveda, Ronen Segev, and Ido Golding. 2011. “General Properties of Transcriptional Time Series in Escherichia Coli.” *Nature Genetics* 43 (6): 554–60.

Surkova, Svetlana, David Kosman, Konstantin Kozlov, Manu, Ekaterina Myasnikova, Anastasia A. Samsonova, Alexander Spirov, Carlos E. Vanario-Alonso, Maria Samsonova, and John Reinitz. 2008. “Characterization of the Drosophila Segment Determination Morphome.” *Developmental Biology* 313 (2): 844–62.

Suter, David M., Nacho Molina, David Gatfield, Kim Schneider, Ueli Schibler, and Felix Naef. 2011. “Mammalian Genes Are Transcribed with Widely Different Bursting Kinetics.” *Science* 332 (6028): 472–74.

Venken, Koen J. T., Joseph W. Carlson, Karen L. Schulze, Hongling Pan, Yuchun He, Rebecca Spokony, Kenneth H. Wan, et al. 2009. “Versatile P[acman] BAC Libraries for Transgenesis Studies in Drosophila Melanogaster.” *Nature Methods* 6 (6): 431–34.

Venken, Koen J. T., Yuchun He, Roger A. Hoskins, and Hugo J. Bellen. 2006. “P[acman]: A BAC Transgenic Platform for Targeted Insertion of Large DNA Fragments in D. Melanogaster.” *Science* 314 (5806): 1747–51.

Warming, Søren, Nina Costantino, Donald L. Court, Nancy A. Jenkins, and Neal G. Copeland. 2005. “Simple and Highly Efficient BAC Recombineering Using galK Selection.” *Nucleic Acids Research* 33 (4): e36.

Warrior, R., and M. Levine. 1990. “Dose-Dependent Regulation of Pair-Rule Stripes by Gap Proteins and the Initiation of Segment Polarity.” *Development* 110 (3): 759–67.

Wilkie, Gavin S., Antony W. Shermoen, Patrick H. O’Farrell, and Ilan Davis. 1999. “Transcribed Genes Are Localized according to Chromosomal Position within Polarized Drosophila Embryonic Nuclei.” *Current Biology: CB* 9 (21): 1263–S6.

Xu, Heng, Leonardo A. Sepúlveda, Lauren Figard, Anna Marie Sokac, and Ido Golding. 2015. “Combining Protein and mRNA Quantification to Decipher Transcriptional Regulation.” *Nature Methods* 12 (8): 739–42.

Xu, Heng, Samuel O. Skinner, Anna Marie Sokac, and Ido Golding. 2016. “Stochastic Kinetics of Nascent RNA.” *Physical Review Letters* 117 (12). https://doi.org/10.1103/PhysRevLett.117.128101.

Yunger, Sharon, Liat Rosenfeld, Yuval Garini, and Yaron Shav-Tal. 2010. “Single-Allele Analysis of Transcription Kinetics in Living Mammalian Cells.” *Nature Methods* 7 (8): 631–33.

Zenklusen, Daniel, Daniel R. Larson, and Robert H. Singer. 2008. “Single-RNA Counting

Reveals Alternative Modes of Gene Expression in Yeast." *Nature Structural & Molecular Biology* 15 (12): 1263–71.
Zoller, Benjamin, Shawn C. Little, and Thomas Gregor. 2018. "Diverse Spatial Expression Patterns Emerge from Unified Kinetics of Transcriptional Bursting." *Cell* 175 (3): 835–47.e25.

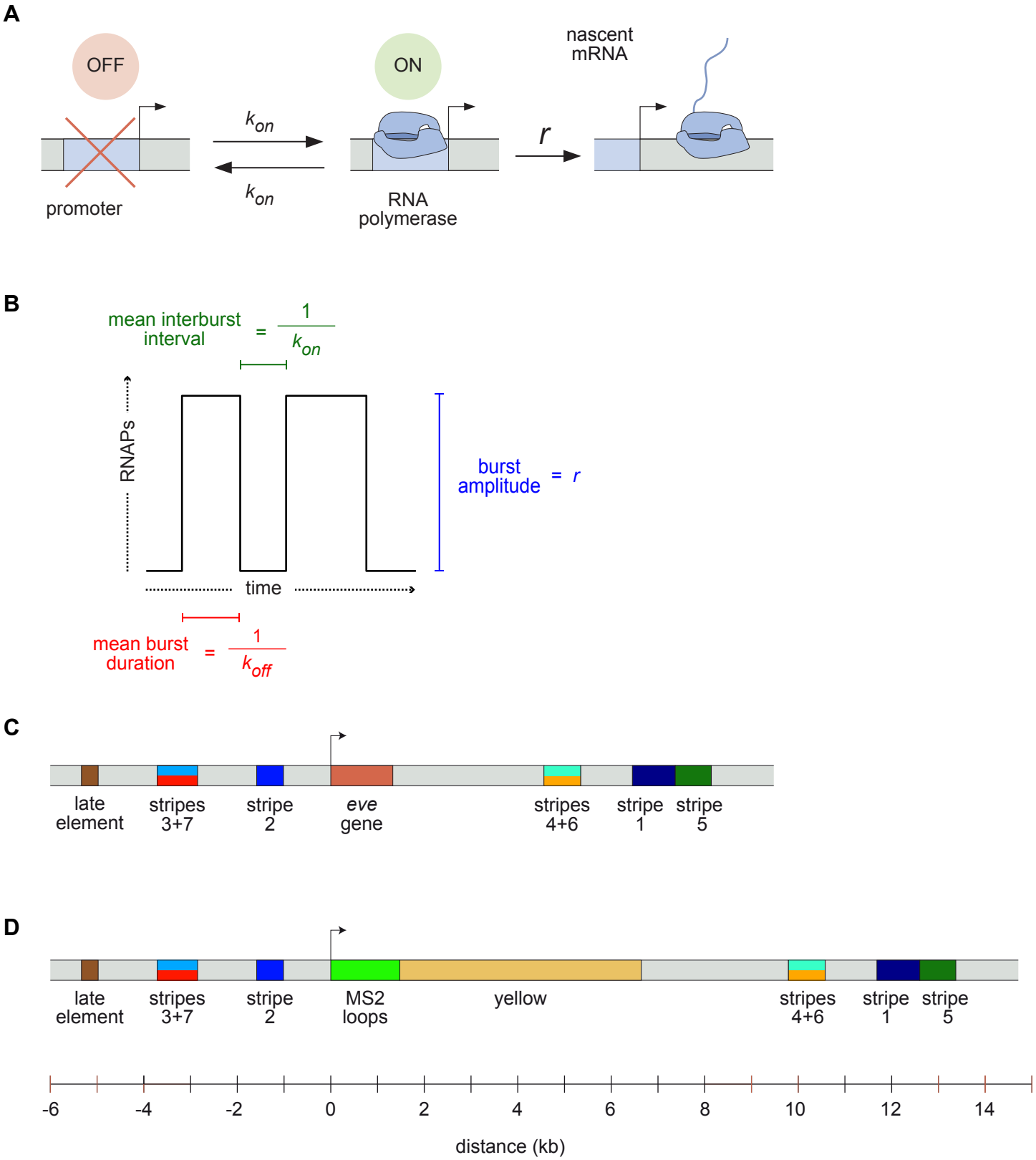

Figure 1. Visualizing live transcription from the seven stripes of *D. melanogaster even-skipped*. (A) Simple model of transcriptional bursting by promoter switching between ON and OFF states. (B) The promoter switching parameters define the burst duration, frequency and amplitude. (C) Wild-type *eve* locus showing the five stripe enhancers (1,2,3+7,4+6,5) and the late enhancer element. Colors for individual stripes are used throughout figures. (D) Layout of the engineered *eve* BAC showing the locations of the MS2 stem loop array and *yellow* gene.

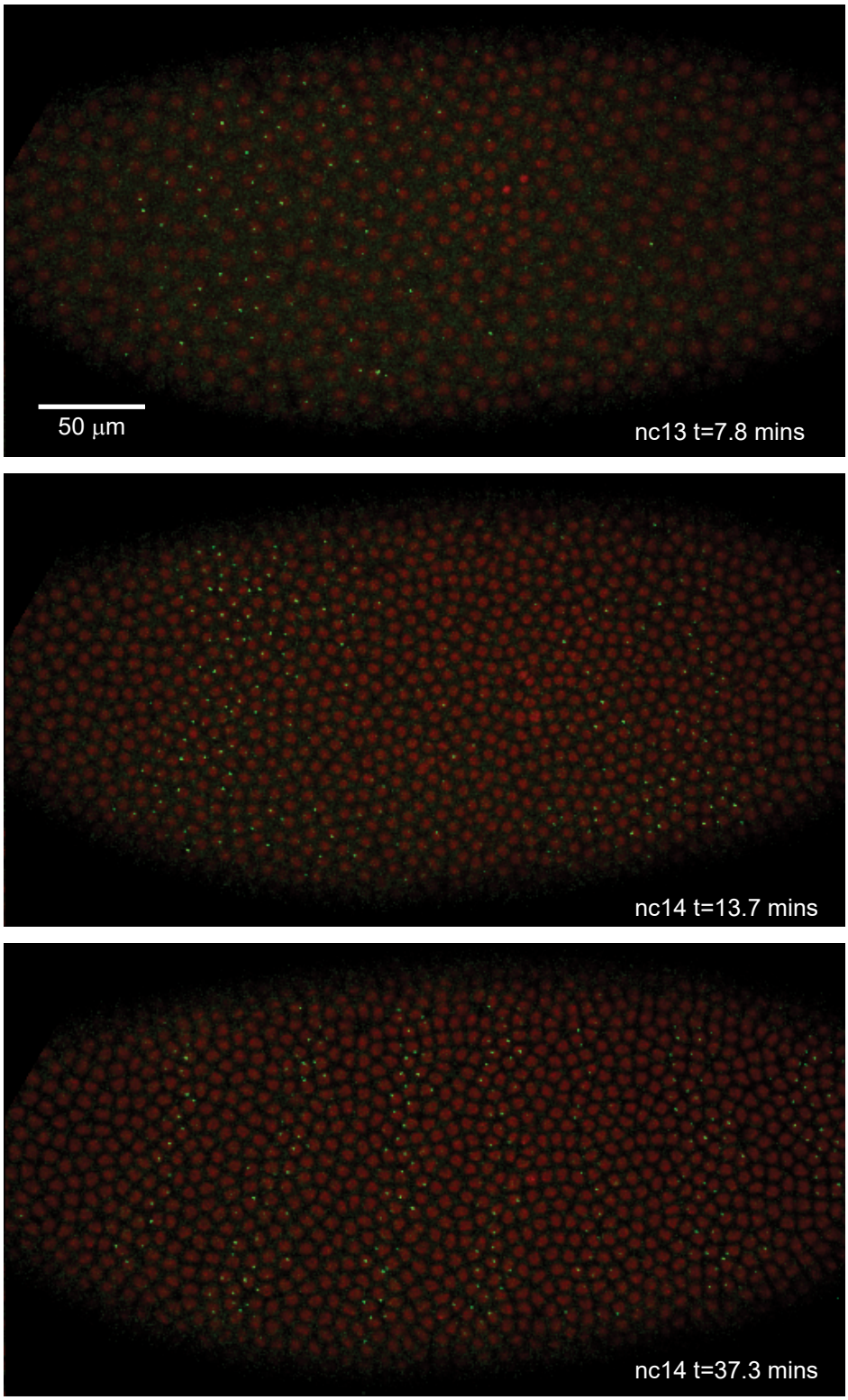

Figure 2. Live expression of even-skipped. Stills from maximum projection renderings of image stacks of an embryo spanning all seven stripes. This movie was collected witha 40x objective for illustration purposes only. Movies used for data analysis were collected at higher resolution as described in the text.

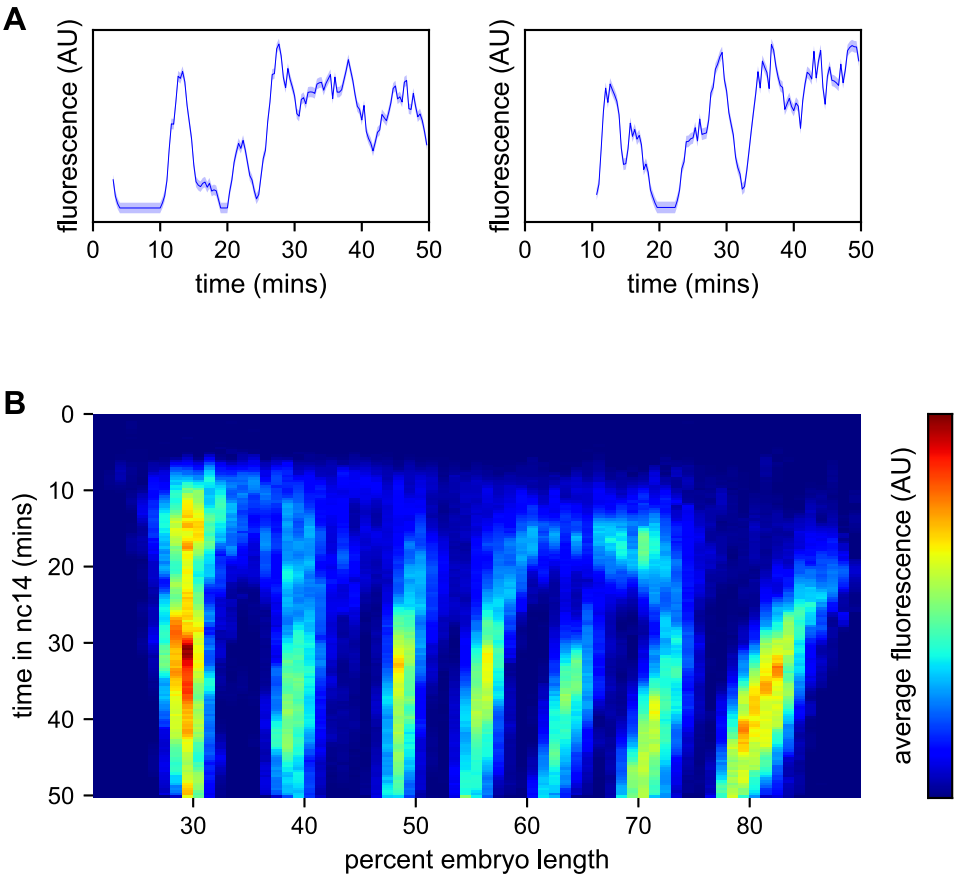

Figure 3. Spatiotemporal dynamics of even-skipped expression. (A) Fluorescence traces from two representative nuclei (particle ID = 1.0163 and 11.0448). (B) Average fluorescence over space and time showing stripe formation, modulation and movement. The time resolution along the y-axis is 20s. The positions of nuclei along the x-axis were registered across movies based on the inferred position of stripe centers, and placed into bins of one percent embryo length, with the average fluorescence of all nuclei in each bin plotted. (A, shading corresponds to the error estimated based on the background fluorescence fluctuations as described in (Garcia et al. 2013)).

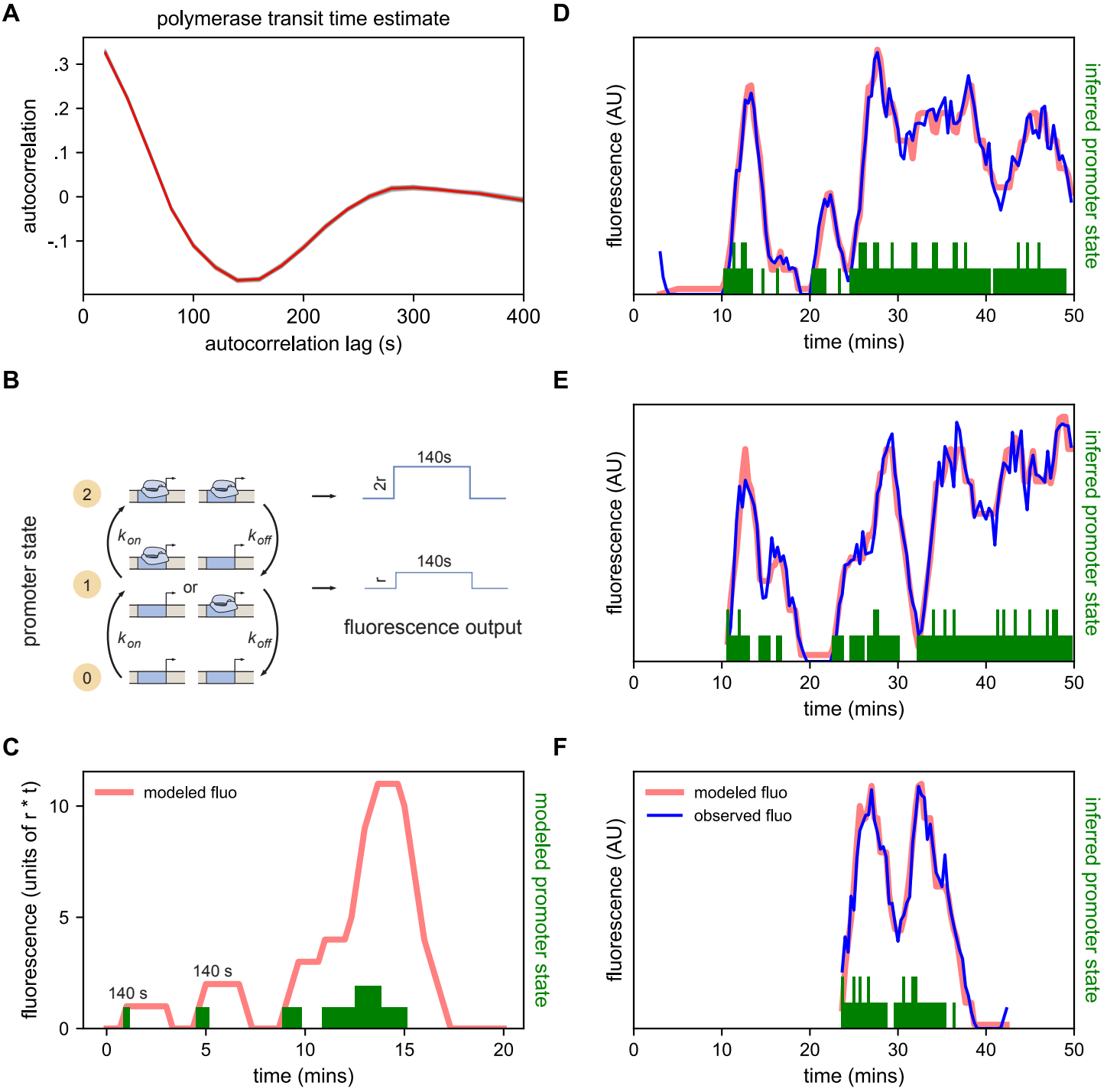

Figure 4. Modeling bursting in individual nuclei. (A) A key parameter in relating fluorescence output to the bursting state of a promoter is the time it takes for a polymerase to transit the gene, which we determined as approximately 140s by examining the autocorrelation (red line) of the change in fluorescence. Gray lines show 100 bootstraps over randomly selected sets of 80% of nuclei; note they almost perfectly overlap the red line. (B) Three state model accounting for post-replication presence of sister chromatids. When either promoter is ON for a short time period Δt, loads polymerases at a constant rate contributing a pulse of polymerase that persists for 140s. (C) Simplified example of the expected observed fluorescence (red line) produced from a hypothetical promoter state sequence. The fluorescence is the sum of the fluorescence pulses produced when one or both promoters are ON (given by the height of the green bars). (D-F) Representative fluorescence traces from individual nuclei (blue lines), inferred bursting pattern (green bars) and fluorescence imputed by cpHMM (red line) for particles 1.0163 (D), 11.0448 (E) and 5.0231 (F).

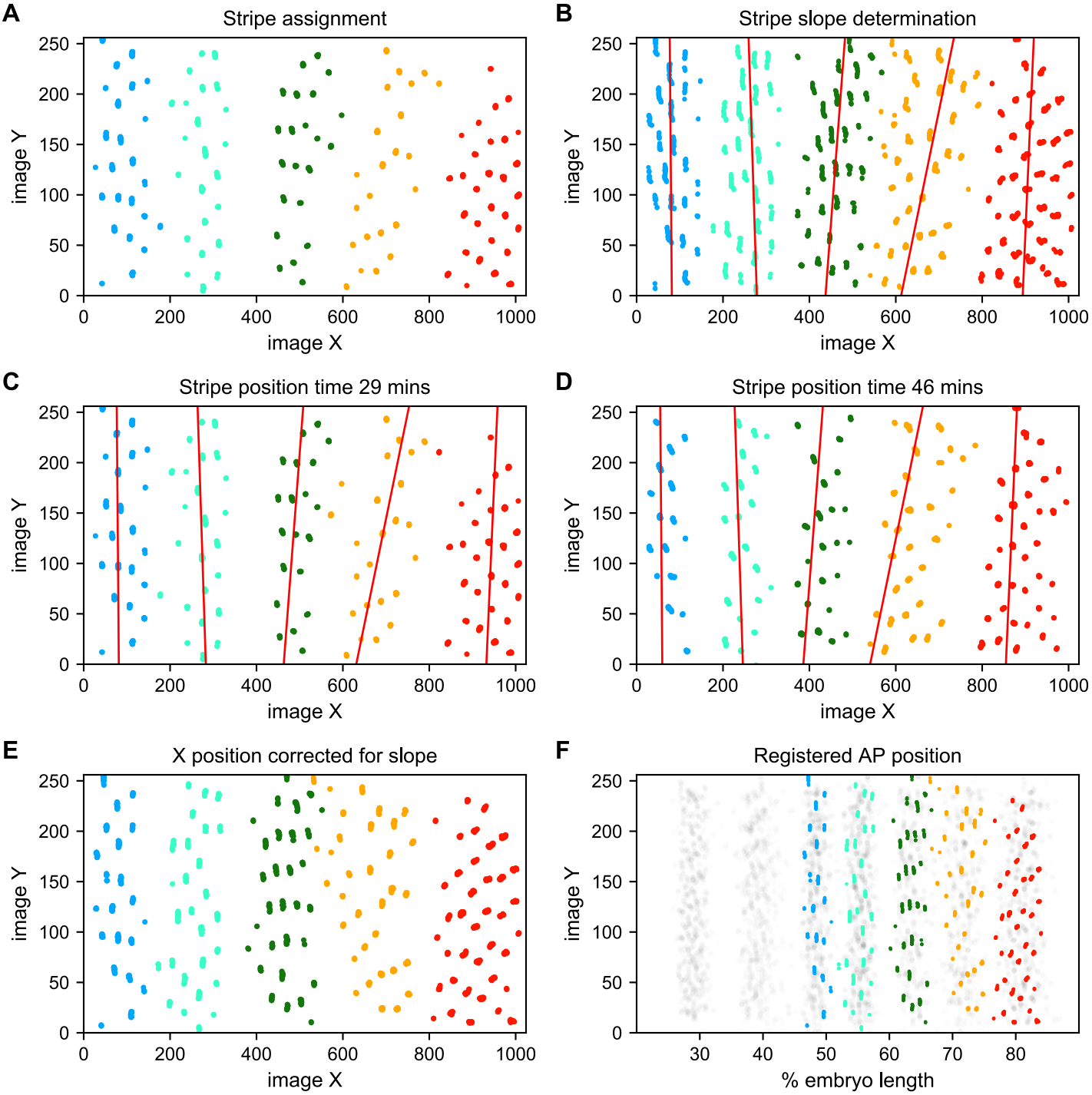

Figure 5. Stripe assignment and alignment. (A) We preliminarily assign bursting nuclei to stripes by applying a Gaussian mixture model to each movie independently in overlapping six-minute time windows with the number of Gaussians equal to the number of stripes captured in that movie. An example is shown here from Movie 2. (B,C,D) We next determine the orientation of each stripe to the imaging axes by fitting a line to coordinates of all nuclei from t > 25 min assigned to that stripe in each movie and time window. (E) We use these fits to generate a linear model of the position of each stripe in each image over time, which makes it possible to reorient the stripe so that it is perpendicular to the image x-axis . (F) The known coordinates of the anterior and posterior poles of the embryo are used to convert the image x-axis to AP position and register the stripes from different movies to each other, as shown here for nuclei from Movie 2 colored by stripe and nuclei corresponding to all other movies drawn in grey.

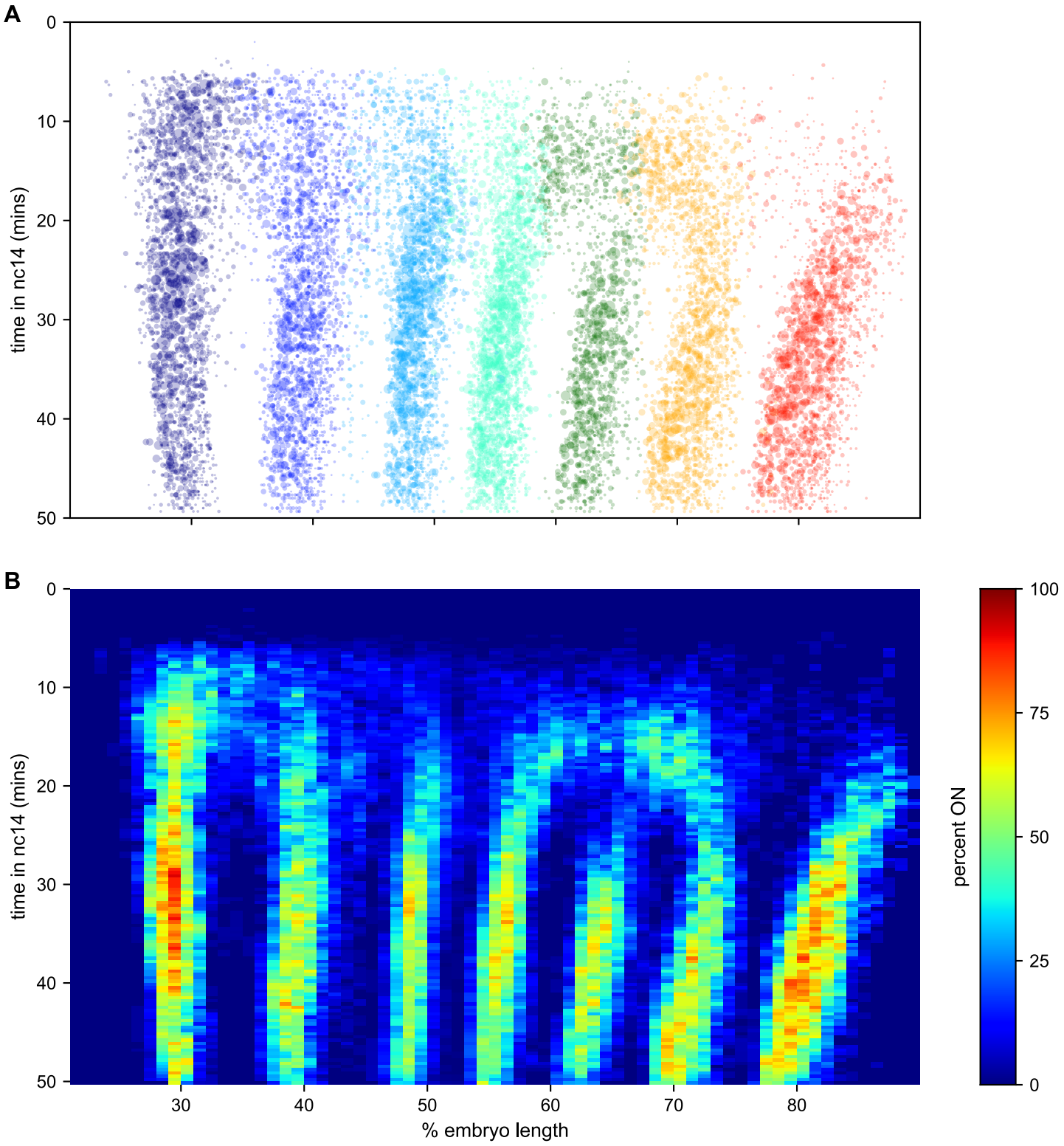

Figure 6. The kinetic fingerprint of *even-skipped* stripe formation. (A) Inferred location of every transcriptional burst in all 11 movies as a function of time and where along the anterio-posterior axis (plotted as fraction of embryo length) each burst occurred. The size of the dot represents the duration of the burst. Collectively the data create a kinetic fingerprint of eve stripe formation. (B) Instantaneous fraction of nuclei in the transcriptionally active ON state as a function of time and position along the embryo.

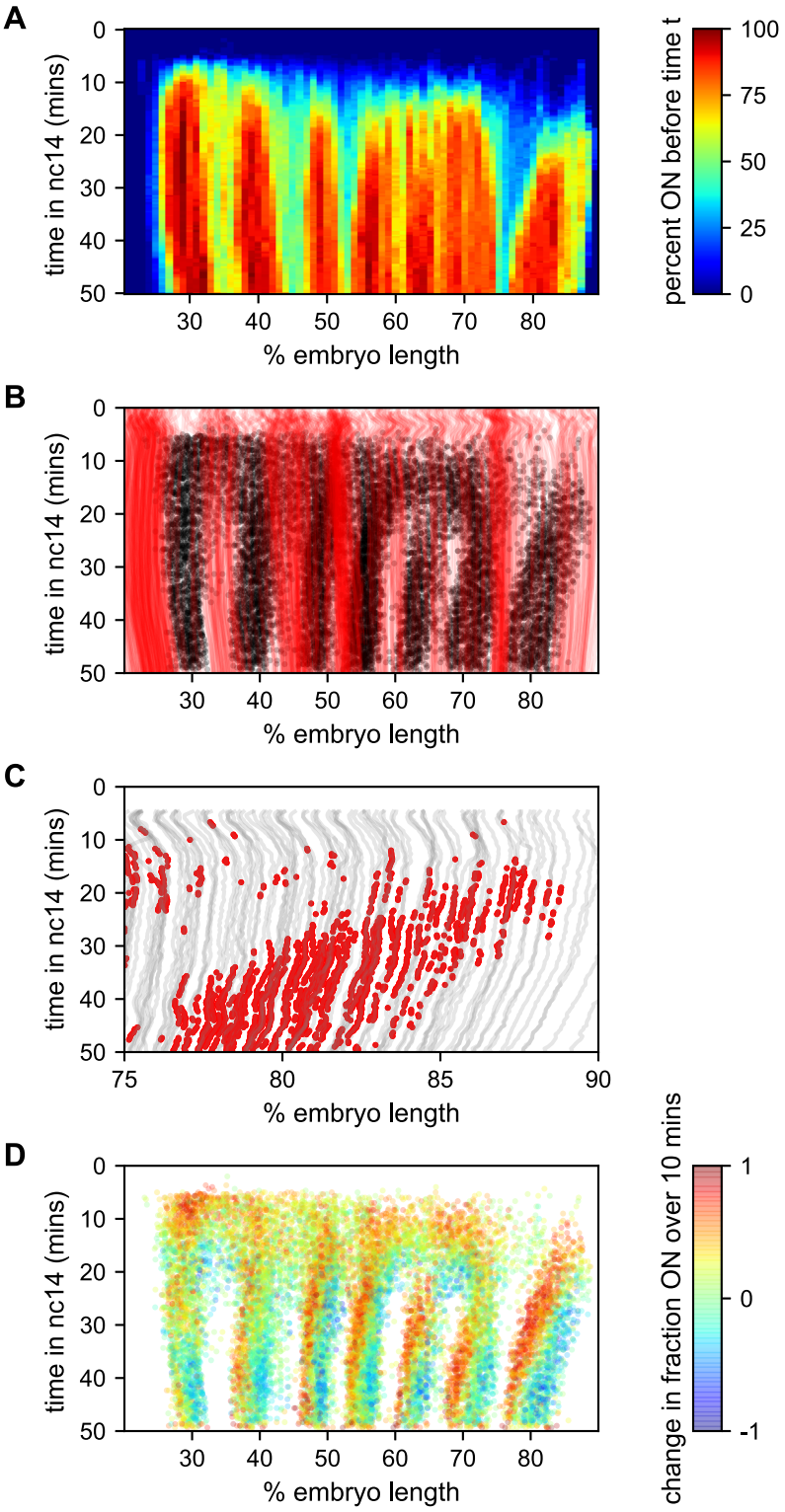

Figure 7. Stripe formation and movement. (A) Fraction of nuclei bursting before time *t* as a function of position along the embryo. (B) Locations of new bursts (black dots) in space and time along with spatiotemporal traces of nuclei that are in the OFF state throughout nc14 (red lines). (C) Traces of nuclei positions over time (gray lines) from stripe 7 region of movie EVE_D6 with timepoints where new bursts initiated colored red to illustrate stripe movement relative to nuclei. (D) Difference in transcriptional activity as defined as the difference between the fraction of the time each nucleus is in the ON state in the subsequent 10 min minus the fraction of time the nucleus is in the ON state in the preceding 10 min. Positive values represent a nucleus turning on or increasing activity, while blue values indicate a nucleus turning off or decreasing activity.

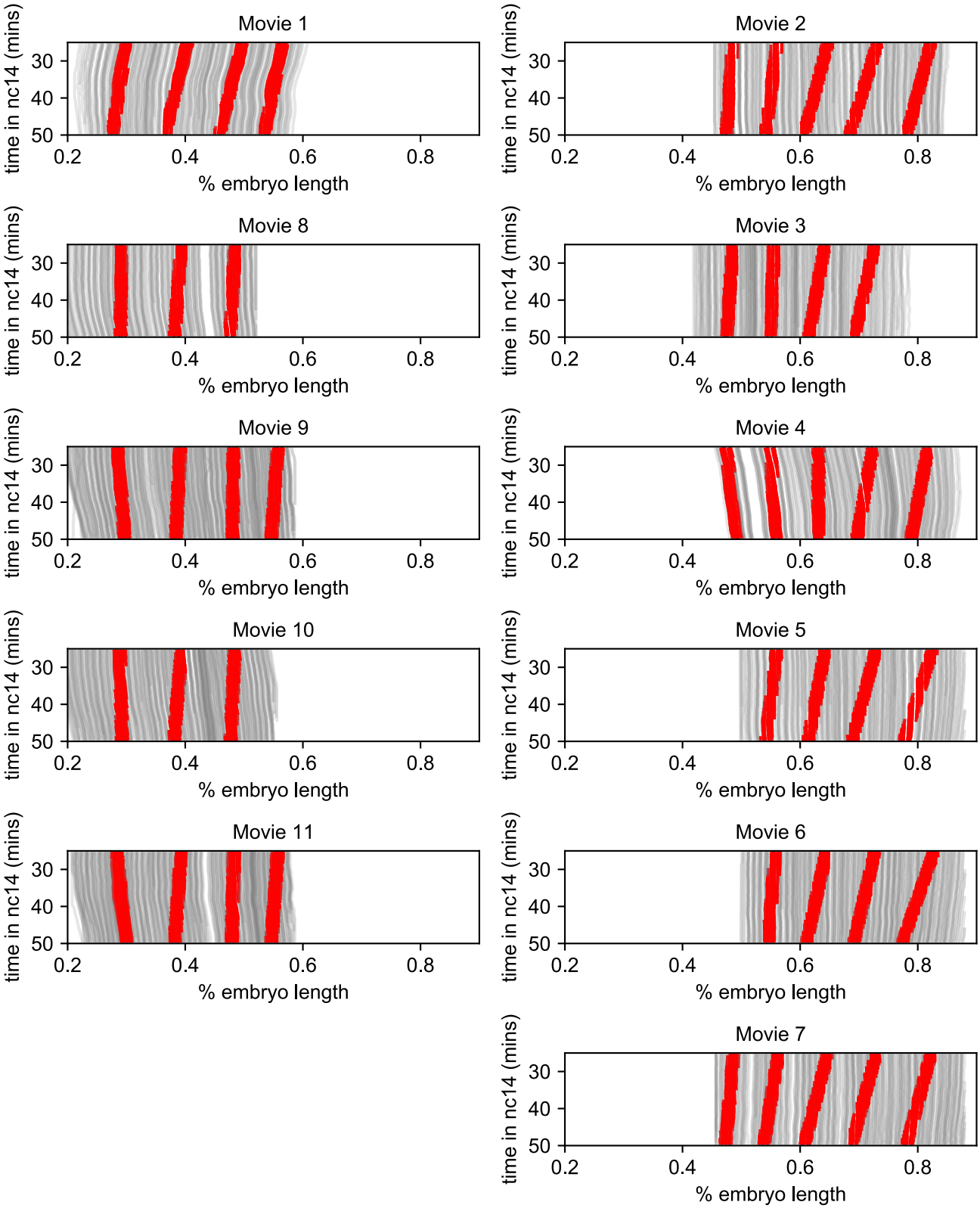

Figure 7-S1. Stripe movement is dominated by the movement of transcriptional activity. Traces of nuclei positions over time (gray lines) from all eleven movies with time points corresponding to transcriptional bursts annotated as in stripes colored red.

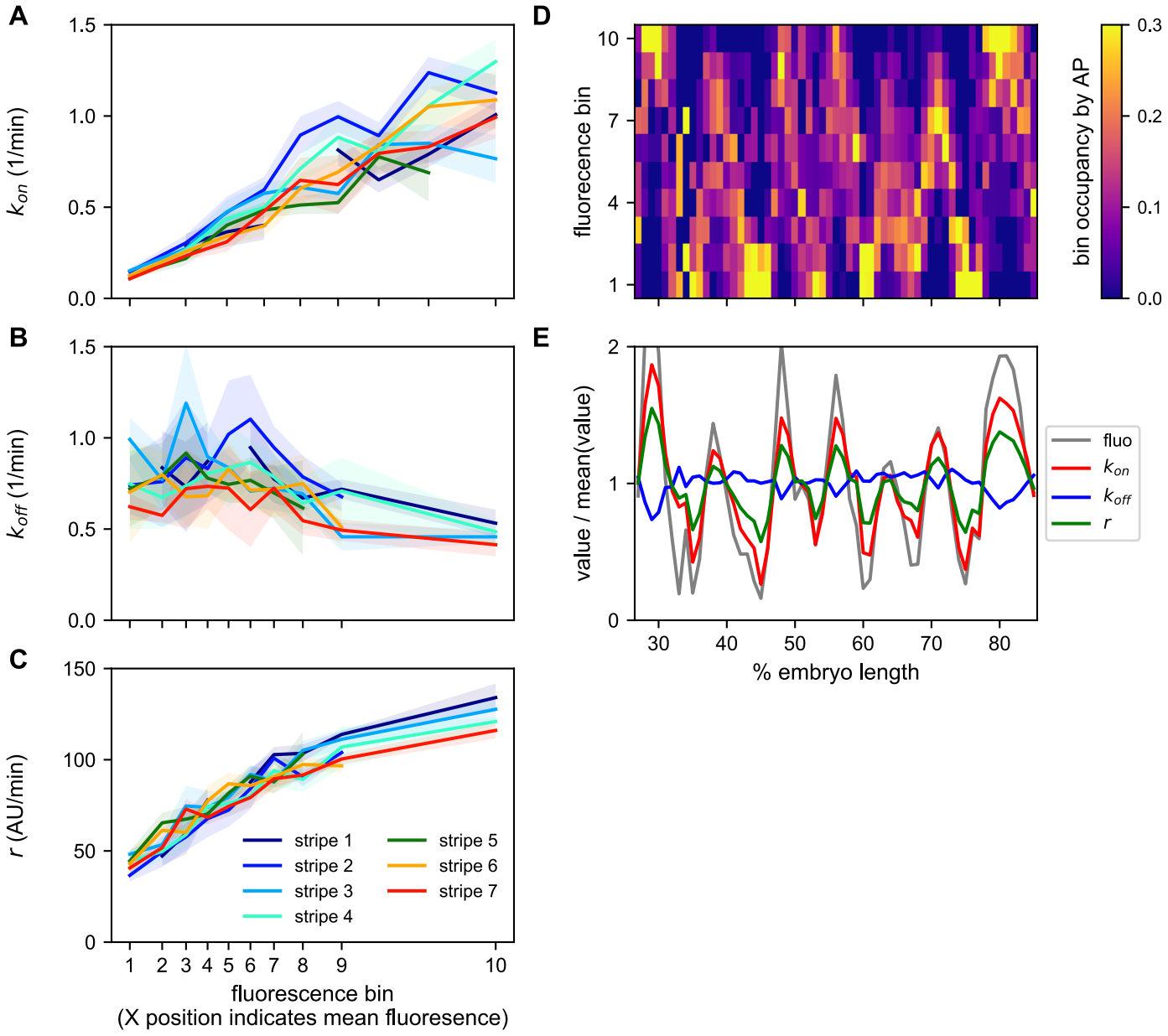

Figure 8. A common bursting control mechanism across all even-skipped stripes. (A-C) cpHMM inference was carried over nuclei binned according to their average fluorescence value indicating that while (A) kon and (C) r are subject to the same regulation along all stripes, (B) koff remains unchanged. Error bars are calculated by taking the standard deviation across cpHMM inference results for multiple bootstrapped samples of experimental data. (D) Distribution of average nuclear fluorescence values along the AP axis. (E) Mean nuclear fluorescence values for each AP position together with the corresponding averaged and weighted bursting parameters.rsting control mechanism across all even-skipped stripes.